# Nonreciprocity of spin waves in noncollinear magnets due to the Dzyaloshinskii-Moriya interaction

Flaviano José dos Santos , <sup>1,2,\*</sup> Manuel dos Santos Dias , <sup>1</sup> and Samir Lounis <sup>1</sup> <sup>1</sup>Peter Grünberg Institut and Institute for Advanced Simulation, Forschungszentrum Jülich and JARA, D-52425 Jülich, Germany <sup>2</sup>Department of Physics, RWTH Aachen University, 52056 Aachen, Germany

(Received 25 March 2020; revised 19 August 2020; accepted 19 August 2020; published 1 September 2020)

Broken inversion symmetry in combination with the spin-orbit interaction generates a finite Dzyaloshinskii-Moriya interaction (DMI), which can induce noncollinear spin textures of chiral nature. The DMI is characterized by an interaction vector whose magnitude, direction, and symmetries are crucial to determine the stability of various spin textures, such as skyrmions and spin spirals. The DMI can be measured from the nonreciprocity of spin waves in ferromagnets, which can be probed via inelastic scattering experiments. In a ferromagnet, the DMI can modify the spin-wave dispersion, moving its minimum away from the  $\Gamma$  point. Spin waves propagating with opposite wave vectors are then characterized by different group velocities, energies, and lifetimes, defining their nonreciprocity. Here, we address the case of complex spin textures, where the manifestation of DMI-induced chiral asymmetries remains to be explored. We discuss such nonreciprocal effects and propose ways of accessing the magnitude and direction of the DMI vectors in the context of spin-polarized or spin-resolved inelastic scattering experiments. We show that only when a periodic magnetic system has finite net magnetization, that is, when the vector sum of all magnetic moments is nonzero, can it present a total nonreciprocal spin-wave spectrum. However, even zero-net-magnetization systems, such as collinear antiferromagnets and cycloidal spin spirals, can have spin-wave modes that are individually nonreciprocal, while the total spectrum remains reciprocal.

## DOI: 10.1103/PhysRevB.102.104401

#### I. INTRODUCTION

In Ref. [1] Anderson discusses the importance of symmetry breaking in nature. Since then, there has been an ever-growing interest in the symmetries and symmetry breaking of condensed-matter systems. An example is the Dzyaloshinskii-Moriya interaction (DMI), which originates from the combination of broken inversion symmetry with the spin-orbit interaction [2,3]. The DMI is a chiral interaction introducing a vector coupling between two spin moments,  $\mathbf{D}_{12} \cdot (\mathbf{S}_1 \times \mathbf{S}_2)$ , which favors one sense of rotation of the spins. Thus, some static and dynamical physical properties of magnetic materials can acquire the chirality of the DMI. For example, spin-polarized scanning tunneling microscopy revealed that spin spirals with a unique rotational sense are present in a single atomic layer of manganese deposited on tungsten [4,5]. Also, when a spin-wave current is driven by a thermal gradient, the DMI can lead to the magnon Hall effect [6]. In ferromagnetic materials, the DMI can impart a fixed chirality to the domain walls, which can then be moved very efficiently with applied currents [7,8], and the domain walls themselves can be seen as fundamental building blocks for magnonic logic [9-11]. Moreover, the DMI is often the stabilizing mechanism for magnetic skyrmions, which are noncollinear spin textures with particlelike properties currently under heavy investigation as potential future bits for data storage devices [12-18]. Whether a skyrmion or an antiskyrmion (spin textures with the same polarity but opposite

vorticity [19]) can be stabilized is determined by the chirality and symmetries of the DMI [20-22]. Thus, the knowledge of the DMI is essential to understand, design, and control many properties of magnetic systems. However, the DMI itself cannot be directly measured. Instead, we observe DMI-dependent properties, which in turn allow us to obtain information about the DMI for a particular system. Therefore, it is crucial to discover better and more complete ways to experimentally characterize this interaction in complex magnetic materials, as a way of exploiting chirality-dependent effects [23].

The theoretical realization that the spin-wave dispersion of ferromagnets can acquire an asymmetry due to the DMI was put forth by Udvardi and Szunyogh [24] and Costa et al. [25]. The key requirement is that the magnetization and the DMI vectors are not perpendicular, which then leads to the nonreciprocity of the spin-wave dispersion (its energy minimum shifts away from the  $\Gamma$  point) (see Fig. 1). This means that the energies of spin waves with wave vectors of equal magnitude and opposite directions are no longer degenerate. However, if the magnetization lies in a plane of mirror symmetry, the spinwave dispersion remains reciprocal for wave vectors along the magnetization direction, as the effective DMI has to vanish in that case, due to Moriya's rules. Other authors have theoretically proposed to characterize the DMI from the spin-wave properties of thin films [26-28]. These seminal papers have opened a route to experimentally probe the DMI in ferromagnetic materials: the strength and chirality of the DMI can be deduced from the measured asymmetry of the spin-wave dispersion, for instance, by fitting the data to a Heisenberg model Hamiltonian. The chirality can be measured because it defines the direction in which the minimum of the spin-wave

<sup>\*</sup>f.dos.santos@fz-juelich.de

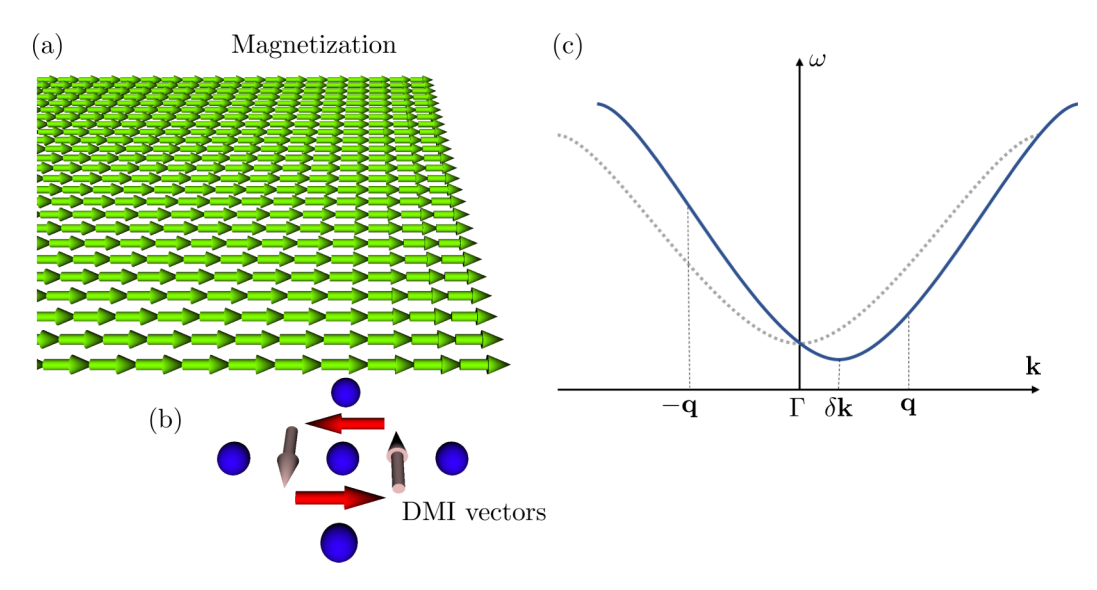


FIG. 1. The shift of the spin-wave dispersion due to the DMI in ferromagnets. (a) In our convention, the magnetization direction of a ferromagnet is given by the direction of the spins. (b) Fragment of a square lattice showing the Dzyaloshinskii-Moriya-interaction vectors between the central atom and its neighbors, all lying in the plane. (c) The DMI components along the magnetization direction, shown in red in (b), induce an asymmetry of the spin-wave dispersion curve, which shifts sideways. Spin waves with opposite wave vectors  $\mathbf{q}$  and  $-\mathbf{q}$  are no longer degenerate, such as in the absence of the DMI (indicated by the gray dotted line). Measuring the location of the new energy minimum  $\delta \mathbf{k}$  provides the chirality (spatial orientation) and magnitude of the DMI.

dispersion shifts away from the  $\Gamma$  point. It is worth mentioning that there are other sources of nonreciprocity, such as dipolar interactions for surface magnetostatic modes [29–31], and the theoretical proposal of combining a noncollinear magnetic structure with an applied external field [32].

There are different experimental techniques able to probe spin waves, such as inelastic scattering with electrons, neutrons, or light, or broadband spectroscopy using coplanar waveguides, each with their capabilities and limitations. In Ref. [33], Zakeri et al. used spin-polarized electron energyloss spectroscopy (SPEELS) [34-38] to experimentally detect the shift of the spin-wave dispersion due to the DMI in thin films of Fe/W(110). The same principles have proven a fruitful way of accessing the DMI when applied to Brillouin light scattering experiments in thin-film systems [39–44] and to inelastic neutron scattering in bulk materials [45–48], with broadband spectroscopy as alternative [49–55]. Similarly, nonreciprocity was observed in antiferromagnets, but only when subjected to an external magnetic field [56]. We have recently proposed spin-resolved EELS (SREELS), which consists of a SPEELS setup augmented with a spin filter for the scattered electrons [57]. Within SREELS, one has access to various spin-scattering channels, where the scattered electrons can either have their spins flipped or not. In contrast to collinear magnets, where only spin-flip processes are responsible for the emission of spin waves, non-spinflip processes can generate spin excitations in noncollinear materials [57].

In this work, we use simple atomistic spin-lattice models to provide a complete characterization of the nonreciprocal effects in the spin-wave spectrum of complex magnetic structures. We show that the angular momentum of a given spin-wave mode can be associated with its handedness, a chirality attribute that allows us to predict the effect of the DMI for that mode. Furthermore, we demonstrate that only

systems with finite total magnetization can feature a nonreciprocal total spin-wave spectrum, e.g., when considering the spin-wave energies of all modes. Moreover, this nonreciprocity is observed on the reciprocal-space directions where the Fourier-transformed DMI vectors have finite projections on the magnetization. In zero-net-magnetization systems, despite the lack of nonreciprocity of the total spin-wave spectrum, we uncover that individual spin-wave modes can be nonreciprocal. These nonreciprocal modes usually come in pairs, each with opposite angular momentum leading to their dispersion curves to shift in opposite directions while keeping the total spin-wave spectrum reciprocal. We also prove that spin-polarized experiments, such as SPEELS, SREELS, or polarized inelastic neutron scattering, can be used to reveal the DMI-induced nonreciprocity of individual spin-wave modes in noncollinear materials. The nonreciprocity in practice leads to an asymmetric scattering rate for opposite wave vectors, which only appears when the probing-beam polarization aligns with a spin-wave angular momentum probing the Fourier-transformed DMI components parallel to them. Furthermore, we show that the angular momenta of the spinwave modes are strongly related to the DMI, that is, they are given not only by the spin configuration, but they are also directly influenced by the DMI itself. Thus, SREELS and SPEELS measurements would allow determining the chirality of the Dzyaloshinskii-Moriya interaction, which could be used to distinguish a skyrmion from an antiskyrmion lattice, for example.

# II. THEORETICAL FRAMEWORK AND MODEL SYSTEMS

To clarify the interplay between the DMI, the ground-state magnetic structure, and the properties of its spin-wave spectrum, we adopt two very simple spin models that allow us

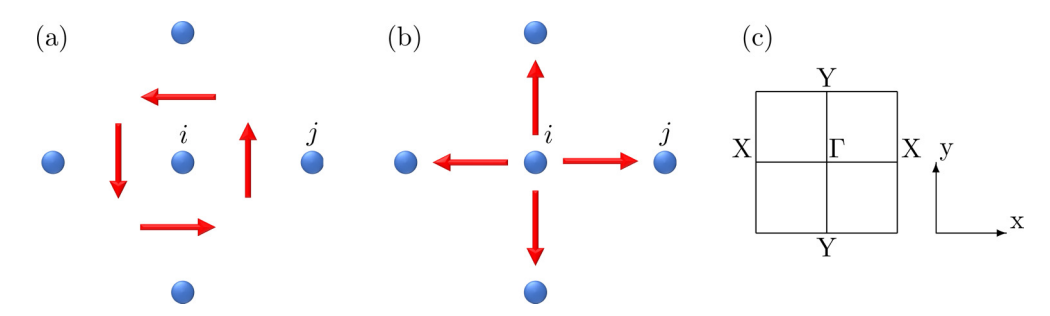


FIG. 2. The two model systems considered in this work. Both consist of a square lattice with nearest-neighbor interactions only. The exchange interaction is the same for both models, but (a) model I has DMI vectors perpendicular to the bonds and swirling counterclockwise, while (b) model II has DMI vectors diverging from the sites being parallel to the bonds. Model I has a cycloidal spin spiral as its ground state, while model II realizes a helical spiral. (c) Brillouin zone with its high-symmetry points and our choice of the frame of reference: The Y- $\Gamma$ -Y path is along  $\hat{\mathbf{y}}$  and X- $\Gamma$ -X is along  $\hat{\mathbf{x}}$ .

to explore all of the involved aspects. These are based on the following generalized classical Heisenberg model, whose Hamiltonian reads as

$$\mathcal{H} = -\frac{1}{2} \sum_{ij} \left( J_{ij} \mathbf{S}_i \cdot \mathbf{S}_j + \mathbf{D}_{ij} \cdot \mathbf{S}_i \times \mathbf{S}_j \right) - \sum_i \mathbf{B} \cdot \mathbf{S}_i, \quad (1)$$

where  $J_{ij}$  is the magnetic exchange interaction parameter,  $\mathbf{D}_{ij}$ is the Dzyaloshiskii-Moriya interaction vector between sites i and j, and **B** is a uniform external magnetic field. We take a square lattice (lattice constant a) for both models, with the magnetic interactions restricted to nearest neighbors. The  $J_{ij}$ are identical in both models (J for all nearest neighbors), but the set of  $\mathbf{D}_{ij}$  vectors differs (note that  $\mathbf{D}_{ji} = -\mathbf{D}_{ij}$ ): model I has typical interfacial DMI vectors perpendicular to the bond connecting the corresponding sites, lying in the plane of the lattice and swirling counterclockwise [see Fig. 2(a)]; model II has bulklike DMI vectors which are parallel to the bonds, also lying in plane and radiating outward from the site i to its neighbors [see Fig. 2(b)]. Figure 2(c) shows the squarelattice Brillouin zone marking its high-symmetry points. For the simulation presented throughout the paper, we took the parameters to be J = 1, D = 1, and S = 1.

We find the ground-state spin configuration for models I and II using atomistic spin dynamics simulations by solving the Landau-Lifshitz-Gilbert (LLG) equation with the SPIRIT code [58]. Using a unit cell of  $8\times 8$  atoms, one obtains for

model I a cycloidal spin spiral [see Fig. 3(a)] and a helical spin spiral for model II [Fig. 3(b)]. In these figures, the wave vector  $\mathbf{Q} = (2\pi/8)\hat{\mathbf{y}}$  of the spin spirals is along  $\hat{\mathbf{y}}$ , however, the spin spirals with wave vector along  $\hat{\mathbf{x}}$  are also possible, which are degenerate to the ones we are showing. By adding an external magnetic field normal to the film in model I, we can stabilize a skyrmion lattice as shown in Fig. 3(c). In this case, the square arrangement of skyrmions is imposed by the choice of the unit cell. The direction of the net magnetization of any spin texture will be denoted by  $\mathbf{n}^0$ .

The spin-wave excitations are computed out of the selfconsistently determined classical ground state in the adiabatic approximation, as explained in detail in Ref. [57]. The classical ground state is specified by a set of spherical angles  $\{\theta_i, \phi_i\}$ which encode the local spin direction on every site. We then construct local coordinate systems for every site with the local z axis coinciding with the classical ground-state spin orientation. The transformation between the global and local frames is given by  $\mathbf{S}_i = \mathbf{R}(\theta_i, \phi_i)\mathbf{S}'_i$ , where  $\mathbf{R}(\theta_i, \phi_i)$  is a rotation matrix. In the local frame, we can expand the quantum spin operators using the linearized Holstein-Primakoff transformation as  $\mathbf{S}_i' = (\sqrt{2S} \frac{a_i + a_i^{\dagger}}{2}, \sqrt{2S} \frac{a_i - a_i^{\dagger}}{2i}, S - a_i^{\dagger} a_i)$ , where  $a_i^{\dagger}$  and  $a_i$ are bosonic ladder operators. Keeping only terms up to second order in the Holstein-Primakoff bosons, the Hamiltonian can be written as  $\mathcal{H} = \mathcal{H}_0 + \mathcal{H}_2$ , where the  $\mathcal{H}_0$  is a constant corresponding to the classical ground-state energy and  $\mathcal{H}_2$ 

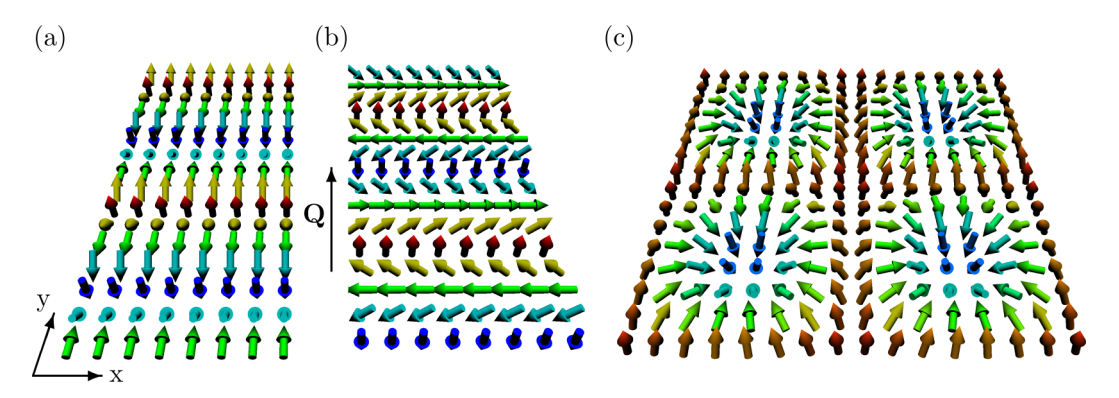


FIG. 3. Spin configuration stabilized by the two models, which assume the MEI and DMI to be limited to the nearest neighbors and J=D=1. (a) A cycloidal spin spiral being the ground state of model I. (b) The helical spin spiral stabilized by model II. Both spin spirals have the same wave vector  $\mathbf{Q} = \frac{2\pi}{8a} \hat{\mathbf{y}}$ . (c) Skyrmion lattice obtained by adding an out-of-plane magnetic field to model I.

contains the quadratic terms of the Holstein-Primakoff bosons describing the spin excitations. The spin-wave eigenvalues  $\omega(\mathbf{k})$  and eigenvectors  $|\mathbf{k}\rangle$  are then obtained by a Bogoliubov transformation, which diagonalizes the system's dynamical matrix in the reciprocal space while ensuring the bosonic character of the diagonalizing basis.

The spin-wave inelastic scattering spectrum is computed with our theory for SREELS of noncollinear magnets discussed in Ref. [57]. We employ time-dependent perturbation theory to describe the interaction between the probing beam and the magnetic system. We arrive to the total dynamical structure factor (summing up all the scattering channels), which is given by

$$\Gamma(\mathbf{q},\omega) \propto \sum_{\alpha} \sum_{\mu\nu} e^{i\mathbf{q}\cdot\mathbf{R}_{\mu\nu}} \mathcal{N}^{\alpha\alpha}_{\mu\nu}(\mathbf{q},\omega),$$
 (2)

where  $\alpha$ ,  $\beta = x, y, z$  and  $\mu$ ,  $\nu$  are site indices for spins in the unit cell that encompasses the noncollinear ground-state magnetic structure. The spin-spin correlation tensor can be expressed using the information about the spin-wave modes as

$$\mathcal{N}_{\mu\nu}^{\alpha\beta}(\mathbf{q},\omega) = \sum_{\mathbf{k},r} \delta[\omega - \omega_r(\mathbf{k})] \langle 0|S_{\mu}^{\alpha}(-\mathbf{q})|\mathbf{k},r\rangle$$
$$\times \langle \mathbf{k}, r|S_{\nu}^{\beta}(\mathbf{q})|0\rangle, \tag{3}$$

where  $\omega_r(\mathbf{k})$  is the energy of the spin-wave mode r with wave vector  $\mathbf{k}$ , and matrix elements of the spin operators between the ground state and the excited spin-wave states [57]. This contains all the information about the spin waves, their signature in the scattering spectroscopy, and also explains the unfolding of the spin-wave modes and the potential extinction of their signal due to destructive interference.

SREELS can also provide spin-resolved spectroscopy of the spin waves. In this setup, a spin-polarized beam of electrons is used to probe the magnetic material (this could be changed to neutrons with little modification). The scattered electrons are then spin filtered with the spin analyzer collinear with the incident beam polarization. This gives rise to four scattering channels, one for each possible combination of (incoming spin)-(outgoing spin). Two of these channels correspond to non-spin-flip processes, namely, the up-up and the down-down channels. The other two, up-down and down-up, account for spin-flip events, where angular momentum is exchanged with the sample.

When probing a ferromagnet with all spins along +z, only the down-up channel can excite spin waves (assuming the probing beam polarization to be parallel to the ferromagnetic magnetization) because this process transfers the exact angular momentum required to excite a quantum of spin wave (the net angular momentum of the spin wave is -1 in units of  $\hbar$ ). In contrast, a spin spiral hosts three types of spin-wave modes (also known as "universal helimagnon modes" [49]). If the beam polarization is aligned perpendicularly to the plane where the magnetic moments rotate in the ground state, their net angular momentum can be inferred from the spin-angular-momentum conservation that defines the four scattering channels in SREELS [57]. One mode appears in the up-down channel and another in the down-up channel, so these are rotational modes with the net angular momentum of

+1 and -1, respectively. The third type of mode appears in the up-up and down-down channels, and so has zero net angular momentum. If the beam polarization is not set as explained, different types of modes can be detected in the same scattering channel.

#### III. RESULTS AND DISCUSSIONS

The following summarizes how the Dzyaloshinskii-Moriya interaction affects the dynamics and energetics of spin waves in collinear and noncollinear magnetic structures followed by extended discussions in the next subsections:

- (A) Nonreciprocal spin-wave spectrum only occurs, in the absence of an external magnetic field, for systems of finite magnetization and when  $\mathbf{n}^0 \cdot \mathbf{D}(\mathbf{k}) \neq 0$ , i.e., if the projection of the Fourier-transformed DMI on the magnetization direction is finite.
- (B) The angular momentum of a spin-wave mode can be regarded as the handedness attribute, which defines the direction toward which the dispersion of the given mode shifts out of the  $\Gamma$  point due to the DMI.
- (C) Systems of zero net magnetization can host spin-wave modes individually nonreciprocal induced by the DMI, while the total spin-wave spectrum remains reciprocal. An external magnetic field can induce nonreciprocity.
- (D) Polarized inelastic scattering experiments can be used to unveil the DMI-induced nonreciprocity, and thus allowing to measure the DMI orientation. A nonreciprocal spectrum only occurs for spin-flip scattering processes due to spin-wave modes whose angular momentum aligns with the polarization of the probing particles and  $\mathbf{D}(\mathbf{k})$ .
- (E) All spin textures that are favored by the DMI have non-reciprocal spin-wave modes with angular momentum aligned to the component of  $\mathbf{D}(\mathbf{k})$  that contributes to the DMI energy gain.

#### A. Nonreciprocal spin-wave spectrum

In the absence of an external magnetic field, a nonreciprocal spin-wave spectrum (different spin-wave energies for modes with wave vectors which are equal in length and opposite in direction) only occurs for systems with finite magnetization. Such a nonreciprocity manifests in the reciprocal-space directions along which a component of  $\mathbf{D}(\mathbf{k})$  aligns with the net magnetization.

The first statement is related to the breaking of time-reversal symmetry. Consider a system described by the Hamiltonian H. If a system is invariant under time-reversal operator  $\Theta$ , then  $\Theta H(\mathbf{k})\Theta^{-1} = H(-\mathbf{k})$ , and the reciprocity of the system is guaranteed. Systems of zero net magnetization, such as antiferromagnets and some spin spirals [e.g., see Figs. 3(a) and 3(b)], are not invariant under time reversal, nor under partial translation  $T_{\lambda/2}$  (translation by half of the spin spiral wavelength  $\lambda$  along the spiral propagation direction), individually. However, they are invariant under a combined operation of time reversal plus partial translation  $\mathcal{S} = \Theta T_{\lambda/2}$ , which leads to  $\mathcal{S}_{\mathbf{k}} H(\mathbf{k}) \mathcal{S}_{\mathbf{k}}^{-1} = H(-\mathbf{k})$  [59]. When the system has a finite net magnetization, it is not possible to find such a combined operation that leaves the Hamiltonian invariant.

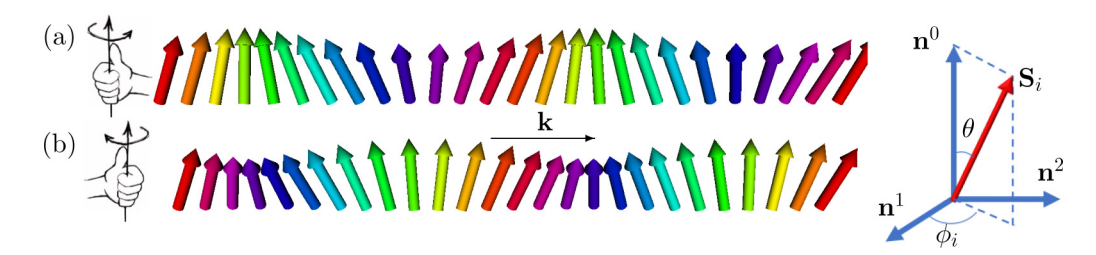


FIG. 4. Instantaneous snapshot of the spin wave of a ferromagnet for a given wave vector  $\mathbf{k}$  as given by Eq. (4). The chirality is defined as the sense in which the spin moments rotation as we proceed along the propagation direction given by  $\mathbf{k}$ . (a) For c=+1, the spin wave has a right-handed chirality. (b) For c=-1, it has a left-handed chirality. The magnetization direction is given by  $\mathbf{n}^0$ . During the precession due to the spin wave, all spins deviate from  $\mathbf{n}^0$  by a fixed angle  $\theta$ . The phase of precession of the *i*th spin is given by  $\phi_i = \mathbf{k} \cdot \mathbf{R}_i$ , where  $\mathbf{R}_i$  is the spin position, and it is used to color code the spins.

We can prove the second statement, following Ref. [24], considering an instantaneous snapshot of a classical spin wave in a ferromagnet, given by

$$\mathbf{S}_i = \cos \phi_i \sin \theta \, \mathbf{n}^1 + c \, \sin \phi_i \sin \theta \, \mathbf{n}^2 + \cos \theta \, \mathbf{n}^0, \quad (4)$$

where  $\mathbf{n}_0$  is a unit vector along the magnetization, which forms an orthonormal basis together with  $\mathbf{n}^1$  and  $\mathbf{n}^2$  (see Fig. 4).  $\theta$  corresponds to a small deviation from the magnetization direction  $\mathbf{n}^0$ , while  $\phi_i = \mathbf{k} \cdot \mathbf{R}_i$  corresponds to a transversal rotation of the spin moments with rotational sense (chirality) given by  $c = \pm 1$ . At this stage, c represents a hypothetical chiral degree of freedom, which we will show later to be fixed by the equations of motion. Placing this expression into Eq. (1), we obtain that the only chirality-dependent term is given by

$$E(\mathbf{k}, c) \propto c \, \mathbf{n}^0 \cdot \mathbf{D}(\mathbf{k}),$$
 (5)

where  $\mathbf{D}(\mathbf{k})$  is the lattice Fourier transform of the Dzyaloshinskii-Moriya vectors. For details on how to obtain the above equation, see the Appendix, Sec. 1.

In both models, the ferromagnetic state can be stabilized by an external magnetic field, but the chiral asymmetry will only manifest when the magnetization has a finite in-plane projection. For model I, the Fourier transformation of the DMI interaction gives  $\mathbf{D}(\mathbf{k}) = 2D[-\sin(ak^y)\hat{\mathbf{x}} + \sin(ak^x)\hat{\mathbf{y}}]$  and, therefore, the asymmetry is strongest for spin waves propagating perpendicularly to the magnetization, and mostly vanishes when parallel to it [see Fig. 5(a)]. For model II, however,  $\mathbf{D}(\mathbf{k}) = 2D[\sin(ak^x)\hat{\mathbf{x}} + \sin(ak^y)\hat{\mathbf{y}}]$  and the asymmetry is strongest mostly for wave vectors parallel to the magnetization [see Fig. 5(b)].

## B. Spin-wave angular momentum and spin-wave handedness

Now we need to establish an important relation between spin-wave chirality, handedness, and angular momentum. In the previous section, our *ansatz* of spin waves considers two possible spin-wave chiralities for a ferromagnet. In the following, we demonstrate that only one of them is a solution to the coupled equation of motions that govern the dynamics. Aside from that, we define a spin-wave handedness, which is a chiral invariant for the spin waves whose sign is related to the direction of the spin-wave dispersion shift in the reciprocal space. Lastly, we show that there is a one-to-one relation

between the spin-wave handedness and the angular momentum. That relation is fundamental in providing an easy and comprehensive way to predict chiral asymmetry in spin-wave dynamics induced by DMI.

Thus far, we know that the spin-wave dispersion curve of a ferromagnet can be shifted out of the  $\Gamma$  point due to the influence of the Dzyaloshinskii-Moriya interactions. This shift was measured in the electron scattering experiments of Zakeri et al. [33], and it occurs toward a very well-defined direction for a fixed direction of the magnetization (given that the DMI is a constant of the material). From this fact, we can infer that spin waves in a ferromagnet have a given handedness that defines how the spin-wave energies respond to the DMI, for example, setting the direction of the dispersion shift. Can a ferromagnet of fixed magnetization host spin waves of opposite handednesses, such that their dispersion curves would shift to the opposite directions? A hint comes from the fact that spin waves in a ferromagnetic system always possess angular momenta along the same direction (antiparallel to the magnetization).

With the previous question in mind, we will review the motion of the spin moments of a ferromagnet when hosting a spin wave. We consider classical spin moments represented by vectors and the phenomenological Landau-Lifshitz equation describing the time evolution of every spin moment:

$$\frac{dS_i(t)}{dt} = -\gamma \mathbf{S}_i(t) \times \mathbf{B}_i^{\text{eff}}(t), \tag{6}$$

where  $\gamma$  is the gyromagnetic ratio. The effective field is given by

$$\mathbf{B}_{i}^{\text{eff}}(t) = -\frac{\partial H}{\partial \mathbf{S}_{i}} = \sum_{j} (J_{ij}\mathbf{S}_{j} + \mathbf{S}_{j} \times \mathbf{D}_{ij}) + \mathbf{B}_{i}, \quad (7)$$

where we considered the Hamiltonian of Eq. (1). We have one equation of motion for each magnetic atom of our material, and these equations are coupled because the effective field in each site depends on the dynamics of the neighboring site to which they couple to via the magnetic interactions.

<sup>&</sup>lt;sup>1</sup>The magnetization, which is the volumetric density of magnetic moment, is antiparallel to spin angular momentum because of the negative electric charge of the electrons. In the literature, however, often the minus sign is disregarded, which is the convention we follow in this paper.

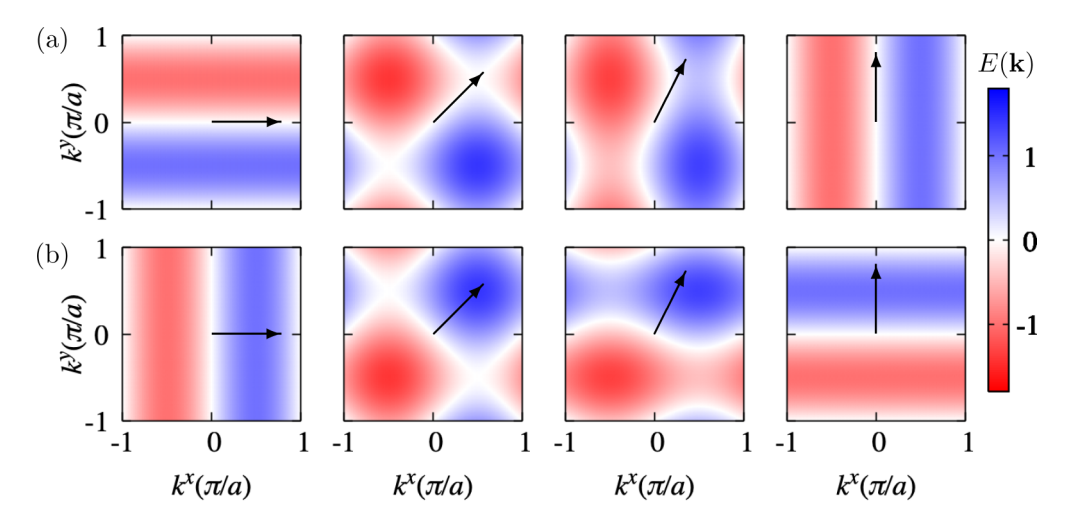


FIG. 5. Chirality-dependent spin-wave energy landscape throughout the Brillouin zone, obtained from Eq. (5). The (a) row corresponds to the energy landscape for model I and row (b) for model II. Each column corresponds to a different in-plane magnetization direction, which is represented by the black arrows.

The presence of the DMI can cause instability in the ferromagnetic phase in favor of the spin-spiral structure. To avoid this problem, we apply a sufficiently large external magnetic field along the z direction. We assume that the spin precession is of small amplitude around its equilibrium direction. The solution steps for the linearized problem are collected in the Appendix, Sec. 1. The time evolution of the spin at site i reads as

$$\mathbf{S}_{i}(\mathbf{k},t) = \frac{1}{\sqrt{N}} \left[ \cos(-\mathbf{k} \cdot \mathbf{R}_{i} + \omega_{\mathbf{k}} t) \,\hat{\mathbf{x}} + \sin(-\mathbf{k} \cdot \mathbf{R}_{i} + \omega_{\mathbf{k}} t) \,\hat{\mathbf{y}} \right] + S \,\hat{\mathbf{z}}, \tag{8}$$

which corresponds to a spin wave of wave vector  $\mathbf{k}$ . Its frequency  $\omega_{\mathbf{k}}$  is given by

$$\omega_{\mathbf{k}} = S(J_0 - J_{\mathbf{k}}^+) + B \quad \text{with} \quad J_{\mathbf{k}} = \sum_{i} A_{ij} \cos(\mathbf{k} \cdot \mathbf{R}_{ij} + \phi_{ij}),$$
(9)

where  $A_{ij} = \sqrt{(D_{ij}^z)^2 + J_{ij}^2}$  and  $\phi_{ij} = \arctan(D_{ij}^z/J_{ij})$ . We have that  $\omega_{\mathbf{k}} \ge 0$  and thus every spin has a counterclockwise precession around the magnetization. In the ferromagnetic ground state, all the spins are aligned, and so the total angular momentum of the system is maximal along  $\hat{\mathbf{z}}$  (the magnetization direction). With a spin wave, as the spins are precessing, the total angular momentum is reduced, which means that the spin-wave angular momentum is antiparallel to  $\hat{\mathbf{z}}$ .

The DMI favors certain cantings between spin moments. Let us then define a spin-wave spatial chirality based on the canting between adjacent spins as the sign of their cross product projected onto the magnetization direction, and integrated over a full revolution of the precessional motion:

$$c_{12}(\mathbf{k}) = \operatorname{sgn}\left(\int_0^{\tau} \hat{\mathbf{z}} \cdot [\mathbf{S}_1(\mathbf{k}, t) \times \mathbf{S}_2(\mathbf{k}, t)]dt\right)$$
$$= -\operatorname{sgn}\left[\sin(a\mathbf{k} \cdot \hat{\mathbf{r}}_{12})\right], \tag{10}$$

where a is the lattice constant and  $\hat{\mathbf{r}}_{12}$  is a unit vector along the bond from site 1 to 2,  $^2$  and  $\tau = 2\pi/\omega_{\mathbf{k}}$  is the precession period. This equation tells us that the chirality changes periodically as a function of  $\mathbf{k}$ , and it is zero for  $\mathbf{k} \cdot \hat{\mathbf{r}}_{12} = n\pi/a$  and particular for  $\mathbf{k} \perp \mathbf{r}_{12}$ . Let us take two wave vectors close to the  $\Gamma$  point, one parallel and another antiparallel to  $\hat{\mathbf{r}}_{12}$ , snapshots of the correspondent spin waves are shown in Figs.  $6(\mathbf{a})$  and  $6(\mathbf{b})$ , respectively. As the DMI favors one of the two chiralities, one of the spin-wave energies is lowered while the other is raised, effectively shifting the energy minimum of the spin-wave dispersion curve out of the  $\Gamma$  point in the direction of  $\mathbf{k}$  that provides the favorable chirality. This shift is what appears as the phase  $\phi$  in Eq. (9).

Next, let us define a more general chirality invariant that does not vary with the wave vector, which we will call the spin-wave handedness:

$$C_{12} = \frac{c_{12}(\mathbf{k})}{\operatorname{sgn}(\mathbf{k} \cdot \hat{\mathbf{r}}_{12})},\tag{11}$$

which is associated with the temporal chirality of a spin wave and has origin in the chirality of the LLG equation itself. Thus, the spin-wave handedness couples to the spin precession sense and to the spin-wave angular momentum. For the spin-wave solution given by Eq. (8), we get  $\mathcal{C}_{12} = -1$ . The direction toward which the spin-wave dispersion shifts couples to the spin-wave handedness. If the handedness were to be +1, instead, the shift would have been in the opposite direction. That is the case if the spin wave were to be given by

$$\mathbf{S}_{i}(\mathbf{k},t) = \frac{1}{\sqrt{N}} \left[ \cos(-\mathbf{k} \cdot \mathbf{R}_{i} + \omega_{\mathbf{k}} t) \hat{\mathbf{x}} - \sin(-\mathbf{k} \cdot \mathbf{R}_{i} + \omega_{\mathbf{k}} t) \hat{\mathbf{y}} \right] - S \hat{\mathbf{z}},$$
(12)

<sup>&</sup>lt;sup>2</sup>Naturally, this definition depends on the choice of the spin pair. It is important to choose a pair such that  $D^{z}(\mathbf{k})$  does not vanish for  $\mathbf{k} \parallel \hat{\mathbf{r}}_{12}$ .

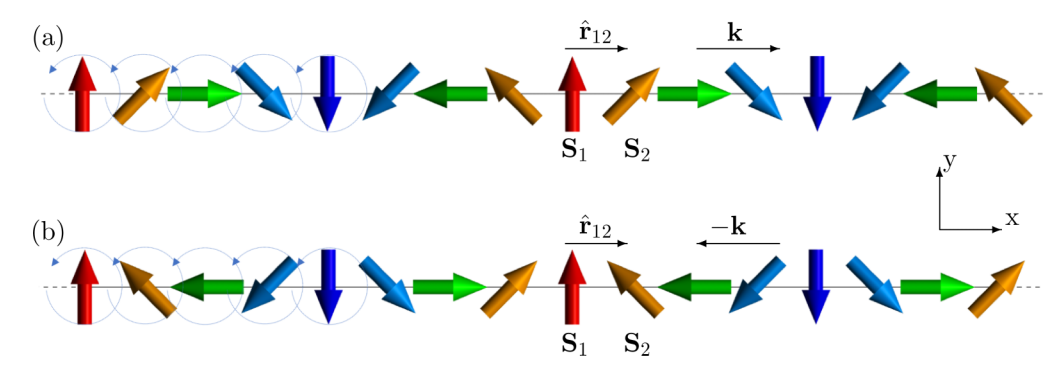


FIG. 6. Spin-wave chirality. In our *ansatz*,  $S^z$  is a constant of motion, therefore, we represent here only the transversal components  $S^x$  and  $S^y$  which change over time. The open circles indicate the precession sense which is fixed by the equation of motion. The precession phase is given by  $\mathbf{k} \cdot \mathbf{R}_i$ . With a spin wave, the system has two inequivalent configurations: (a) one if the wave vector is parallel to  $\hat{\mathbf{r}}_{12}$  yielding  $c_{12} = -1$  (moving from the left to the right, the tilt direction is given by left-hand thumb rule); (b) another if the wave vector is antiparallel to  $\hat{\mathbf{r}}_{12}$ , which results in  $c_{12} = +1$  (the tilt direction is given by right-hand thumb rule).

which corresponds to a clockwise rotation and an angular momentum parallel to  $\hat{\mathbf{z}}$ . Then, we would have  $\mathcal{C}_{12}=+1$ . Thus, a change of handedness comes together with an inversion of the angular momentum, and the dispersion shift due to DMI will occur in the opposite direction of that for spin waves with handedness  $\mathcal{C}_{12}=-1$ . By the way, this second solution corresponds in fact to the spin waves for a ferromagnet with the magnetization along  $-\hat{\mathbf{z}}$ . This momentum-handedness coupling is imposed by the equation of motion that accepts only wavelike solutions.

As we will demonstrate in the following, this linking between angular momentum and handedness also holds for noncollinear magnetic systems, where the spatial chirality can be rather difficult to track. Nevertheless, often these systems have excitations of very well-defined angular momentum, which will then allow us to infer their handedness and thus their response to the DMI. This result is very powerful in allowing us to predict the effect of the DMI on the spin-wave energy and vice versa, as we demonstrate next.

#### C. External magnetic field and zero-net-magnetization systems

Previously, we argued that only systems with finite net magnetization can produce a nonreciprocal spin-wave spectrum due to DMI. Something analogous to that also happens for systems of zero net magnetization: the Dzyaloshinskii-Moriya interaction can induce chiral asymmetries in those systems too. However, it can now only break the chirality degeneracy between rotational spin-wave modes but leaving the total spectrum reciprocally symmetric in the absence of an external magnetic field.

Let us then consider an antiferromagnet, and that the D(k) aligns with the axis of the magnetic moments of the systems. We can regard the antiferromagnet as a superposition of two coupled ferromagnetic sublattices of opposite magnetization. Such a system has two spin-wave modes, each one with angular momentum aligned to one of the sublattice magnetizations. In ferromagnets, flipping the entire magnetization makes the DMI-induced asymmetry to reverse in the reciprocal space [33]. Thus, the antiferromagnet spin waves of opposite angular momenta are shifted in opposite directions, which effectively leaves the total spectrum of the

system reciprocal. The system becomes nonreciprocal once again under the action of an external magnetic field parallel to the alignment axis of the magnetic moments [47,56,60]. And here we have the first mean though which one can reveal the asymmetry induced by DMI in systems of zero net magnetization.

#### D. Role of spin-polarized and -resolved inelastic scattering

Now, we know that DMI can induce hidden chiral asymmetry in the spin-wave spectrum in a system of zero net magnetization and that an external magnetic field can be used to reveal it. We proceed by demonstrating that in the absence of an external magnetic field, we still can identify these asymmetries utilizing spin-polarized and -resolved scattering experiments.

Often, zero-magnetization systems, such as spin spirals and antiferromagnets, host spin-wave modes that come in pairs, where the counterpartner has opposite angular momentum, and therefore, opposite handedness, e.g., two rotational modes of opposite angular momentum. In the absence of DMI, these modes are degenerate and reciprocally symmetric, which would be the case of the two modes in an antiferromagnet. But, as we have seen in the previous subsection, this degeneracy can be lifted by the DMI, leaving each mode nonreciprocal while the total spectrum remains reciprocal. As we have also seen, an external magnetic field couples differently to each mode, energetically favoring one and disfavoring the other, which generates an overall nonreciprocal spectrum [56].

An alternative way to couple with the angular momentum of the spin waves is utilizing spin-resolved scattering experiments, such as SREELS [57]. In the example of an antiferromagnet, this would allow us to measure each mode separately by aligning the polarization of the probing particles to the precession axis of one of the spin-wave modes and measuring only the spin-flip channel. Similarly, the same perfect mode selection can be achieved for spin-spiral systems [57]. This makes of spin-polarized or -resolved inelastic scattering a second means through which one can reveal the DMI-induced nonreciprocity on the spin-wave spectrum.

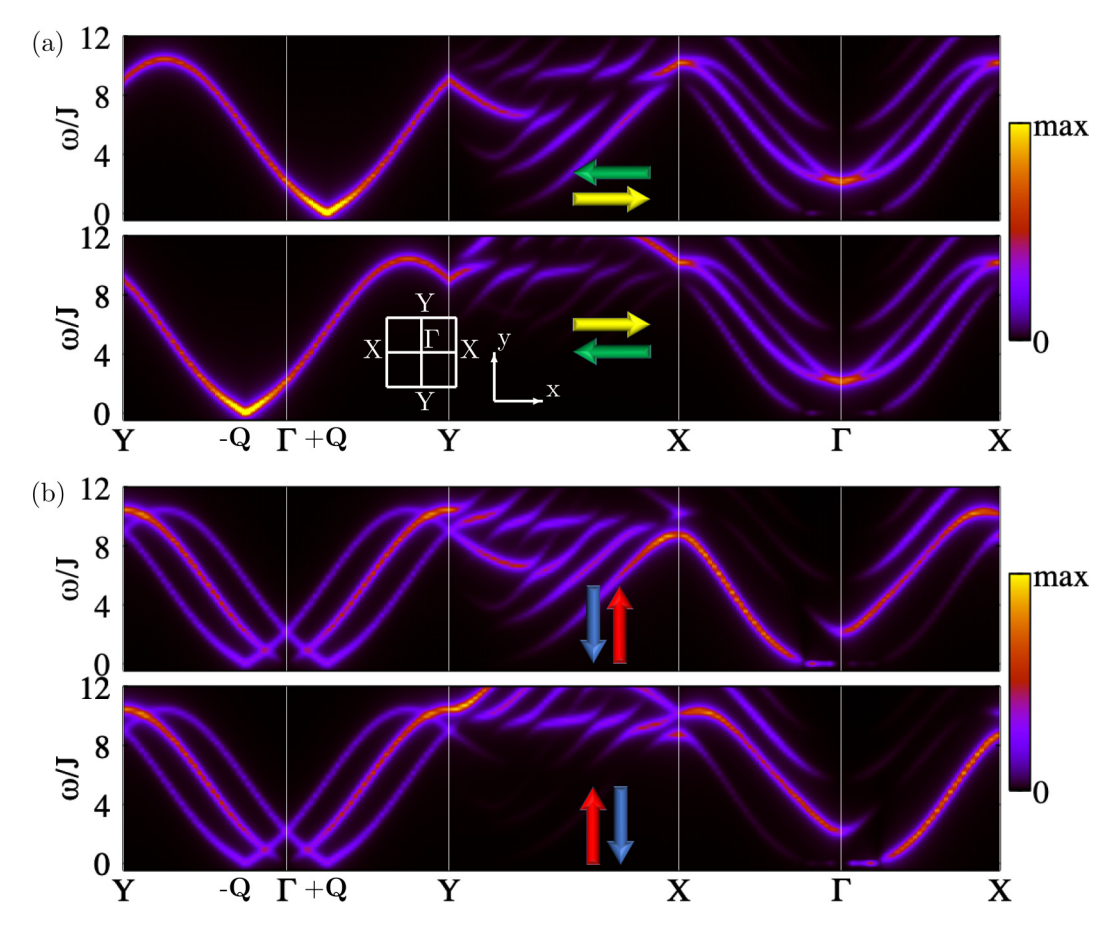


FIG. 7. Spin-resolved inelastic scattering spectra for the spin spiral generated from model I. (a) Shows the two spin-flip channels for polarization along  $\hat{\mathbf{x}}$ , as indicated by the horizontal arrows. Nonreciprocity occurs in the reciprocal space where a component of  $\mathbf{D}(\mathbf{k})$ , polarization, and angular momentum align with each other. For model I on path Y- $\Gamma$ -Y,  $\mathbf{D}(\mathbf{k})$  and the angular momentum of the spin-wave modes with minima at  $\mathbf{k} = \pm \mathbf{Q}$  are parallel to  $\hat{\mathbf{x}}$ . (b) Shows the case for the polarization along  $\hat{\mathbf{y}}$ , indicated by the vertical arrows. Thus, nonreciprocity is only seen in the X- $\Gamma$ -X, when  $\mathbf{D}(\mathbf{k}) \parallel \hat{\mathbf{y}}$  that couples to the angular momentum of those spin waves.

Next, we conjecture the conditions that rule the occurrence or not of nonreciprocal spin-wave spectra in inelastic scattering experiments:

- (i) Nonreciprocal spectrum only occurs for spin-wave modes of finite angular momentum. This is a generalization of the requirement that a system needs a finite magnetization to feature a total nonreciprocal spin-wave spectrum induced by DMI in subsection A. However, this general rule applies to zero-net-magnetization systems. As we have seen, angular momentum translates into the chiral handedness of the spin wave. Without angular momentum, a spin wave is nonchiral and cannot manifest nonreciprocity due to DMI.
- (ii) Only spin-flip channels may present a nonreciprocal spectrum. This is a direct consequence of (i). If only modes of finite angular momenta can be nonreciprocal, and usually these modes are paired to modes of opposite angular momenta, only in a spin-flip channel we can measure one disregarding the other.
- (iii) Only the component D(k) parallel to the spin-wave angular momentum can influence its nonreciprocal spectrum.
- (iv) Only a scattering experiment with the polarization of the probing particles aligned along the spin-wave angular momentum can reveal the nonreciprocity of this mode.

Next, we demonstrate and exemplify items (iii) and (iv) by calculating the spin-resolved spectra for the spin spirals that result from models I and II, introduced in Sec. II, with  $\mathbf{Q} \parallel \hat{\mathbf{y}}$ , shown respectively in Figs. 7 and 8. Model I stabilizes a cycloidal spiral whose spins lay in the *y-z* plane [see Fig. 3(a)], while model II leads to a helical spiral with spins lying in the *x-z* plane [see Fig. 3(b)].

Figure 7(a) shows the spin-flip channels for polarization along  $\hat{\mathbf{x}}$  (represented by horizontal arrows), which present a nonreciprocal spectrum in the Y- $\Gamma$ -Y path, i.e., in a reciprocal-space direction perpendicular to the polarization. For model I,  $\mathbf{D}(\mathbf{k}) = -2D \sin(ak^y)\hat{\mathbf{x}}$  on this path and, therefore, it is parallel to the polarization and to the angular momentum of the spin-wave modes whose energy minima are at  $\mathbf{k} = \pm \mathbf{Q}$ . For Fig. 7(b), the polarization is set along  $\hat{\mathbf{y}}$  (represented by vertical arrows), and nonreciprocity is only seen for the X- $\Gamma$ -X path, again because on this path  $\mathbf{D}(\mathbf{k}) = 2D \sin(ak^x)\hat{\mathbf{y}}$  is parallel to the polarization and the angular momentum of some spin-wave modes. Naturally, a polarization along z will not feature any nonreciprocity because the DMI model has no component along that direction.

For model II, the Fourier-transformed DMI vector on path  $Y - \Gamma - Y$  is  $\mathbf{D}(\mathbf{k}) = 2D \sin(ak^y)\hat{\mathbf{y}}$ , and along  $X - \Gamma - X$  it is  $\mathbf{D}(\mathbf{k}) = 2D \sin(ak^x)\hat{\mathbf{x}}$ . Thus, in contrast to model I, we will

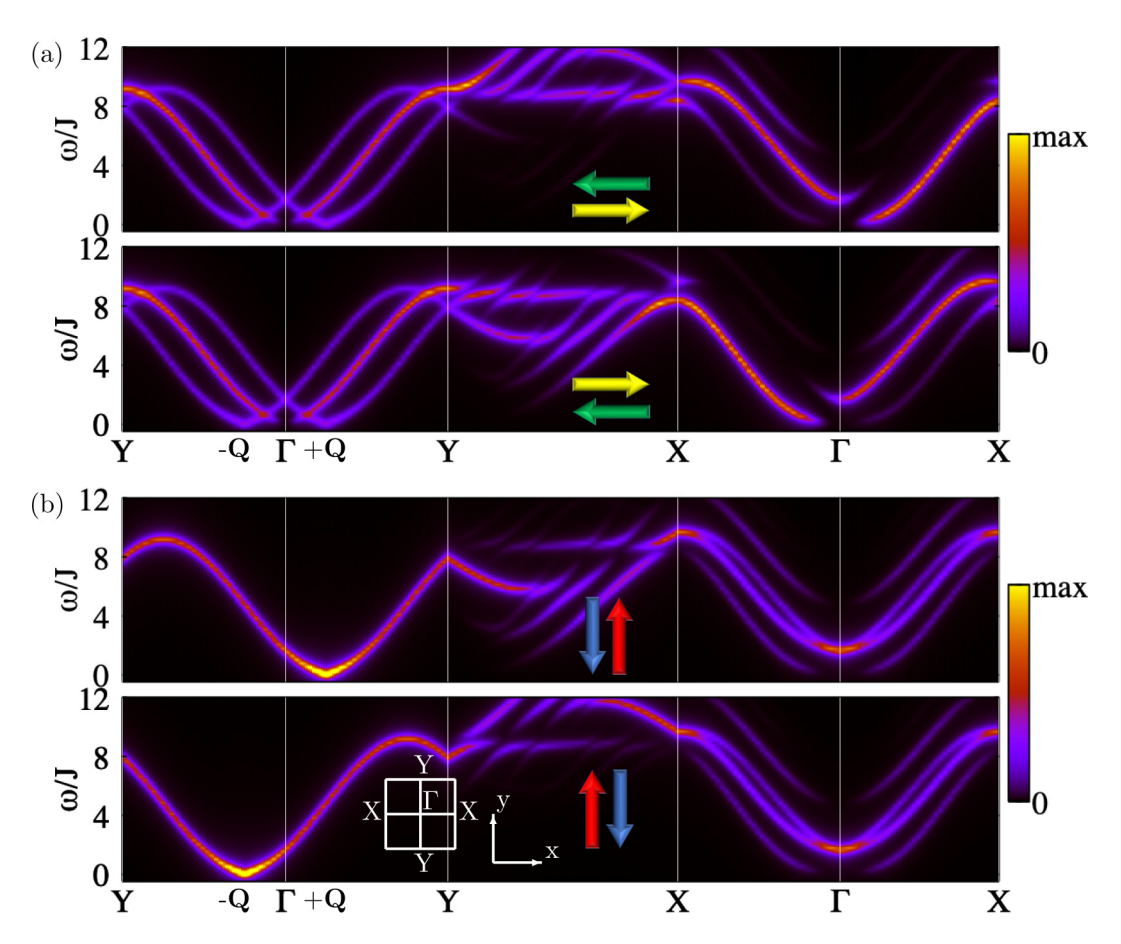


FIG. 8. Spin-resolved inelastic scattering spectra for the spin spiral generated from model II. (a) Shows the two spin-flip channels for polarization along  $\hat{\mathbf{x}}$ , as indicated by the horizontal arrows. Nonreciprocity occurs in the reciprocal space where a component of  $\mathbf{D}(\mathbf{k})$ , polarization, and angular momentum align with each other. For model II on path X- $\Gamma$ -X,  $\mathbf{D}(\mathbf{k})$  and the angular momentum of some spin-wave modes are parallel to  $\hat{\mathbf{x}}$ . (b) Shows the case for the polarization along  $\hat{\mathbf{y}}$ , indicated by the vertical arrows. Thus, nonreciprocity is only seen in the Y- $\Gamma$ -Y, when  $\mathbf{D}(\mathbf{k}) \parallel \hat{\mathbf{y}}$  that couples to the angular momentum of the spin-wave modes whose energy minima are at  $\mathbf{k} = \pm \mathbf{Q}$ .

observe the nonreciprocity on the reciprocal-space direction parallel to the polarization [see Figs. 8(a) and 8(b)], where the polarization is along  $\hat{\mathbf{x}}$  and  $\hat{\mathbf{y}}$ , respectively. In both models, the spin-spiral wave vector points along the same direction, but the direction where the nonreciprocity occurs changes from one model to the other, which shows that the direction of the spiral wave vector has no role on the nonreciprocity.

For more complex systems with lower symmetries, such as skyrmion lattices, the spectrum of each spin-wave mode is not well defined throughout the reciprocal space in inelastic scattering experiments. The spectra are closer to a continuum of excitations instead of the well-separated branches seen for the spin-spiral configurations (see Fig. 9), whereupon adding an out-of-plane external magnetic field to model I could stabilize a skyrmion lattice in an  $8 \times 8$  atoms unit cell [see also Fig. 3(c)]. Naturally, it is also hard to identify the direction of the angular momentum of the underlying spin wave corresponding to each high-intensity region of the spectrum. Nevertheless, the nonreciprocity is still present and measurable. In Fig. 9, we observe a nonreciprocity on the same path,  $Y-\Gamma-Y$ , as seen for the spin spiral established in the absence of the external magnetic field [see Fig. 7(a)], for the same polarization along  $\hat{\mathbf{x}}$ . Even though the two systems look rather different from each other, the reciprocity on their

spectra occurs under the same condition because they share the same DMI structure.

As we have demonstrated, only spin-flip channels can present a nonreciprocal spectrum. However, not always a spin-resolved inelastic scattering experiment is available, as is currently the case of electron scattering setup to study spin waves. A more easily accessible experiment is the spin-polarized setup, where a source of spin-polarized particles is used to scatter from the magnetic material and the spin of the scattered particle is not measured. The resulting spectrum is equivalent to the addition of a spin-flip and a non-spin-slip channel, e.g., down-up plus down-down. While the latter cannot be nonreciprocal, the first can and so is their sum.

Figure 10 represents constant wave-vector spectra, which are the typical measurements done in inelastic electron and neutron scattering experiments. The wave vector of the spin excitations is fixed by controlling the ratio between the incident and scattering angles, and the intensity corresponds to the number of probing particles that have transferred a given amount of energy to the excitations in an interval of time. We calculated the spectra for wave vectors opposite to each other in the reciprocal space  $\mathbf{k} = \pm 2\pi k \hat{\mathbf{y}}$ , and the polarization was set along the  $\hat{\mathbf{x}}$  direction, which aligns with  $\mathbf{D}(\mathbf{k})$ . Figure 10(a) shows the results for a spin-resolved setup

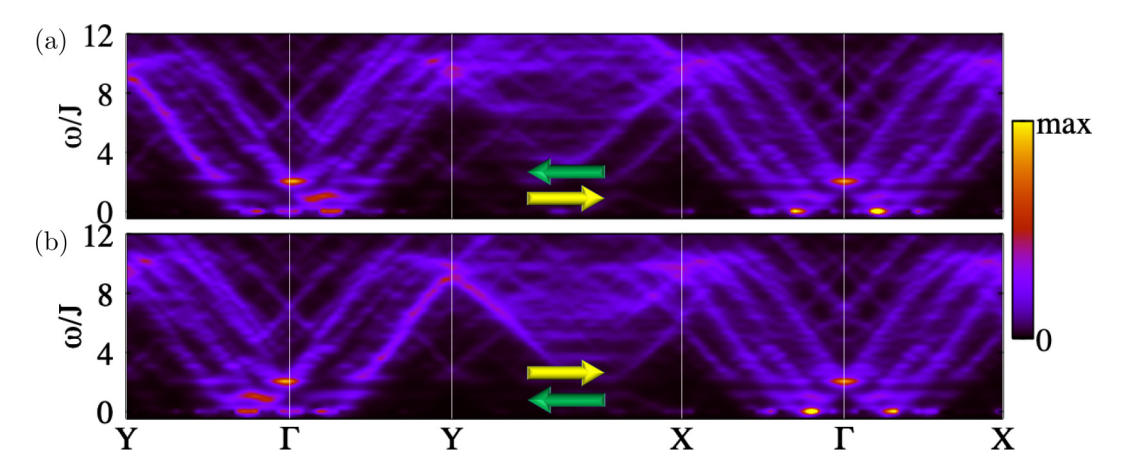


FIG. 9. Spin-resolved inelastic scattering spectra for a skyrmion lattice generated by model I added with an out-of-plane external magnetic field. (a) Represents the left-right spin-flip channel, and (b) shows the right-left one, as indicated by the horizontal arrows. The beam polarization is along  $\hat{\mathbf{x}}$ . The spectra resemble a continuum of excitations rather than well-defined dispersing lines. Nevertheless, the nonreciprocity is visible (along the Y- $\Gamma$ -Y path for this beam polarization), and their occurrence conditions match those for the spin spiral established by the same DMI model in the absence of the external field [see also Fig. 7(a)].

[which corresponds to a vertical line of the spectrum shown in Fig. 9(a)], while Fig. 10(b) presents the spin-polarized spectrum. In the low-energy region, we clearly observe for both setups, spin resolved or spin polarized, a difference in the scattering intensity. For higher energies, some peaks vanish and others appear when comparing the spectra for the two opposite wave vectors.

It is the DMI directional sense that determines which scattering intensity will be higher, at  $+\mathbf{k}$  or  $-\mathbf{k}$ . Upon reversing the DMI, the spectra would be swapped in Fig. 10. This implies that such an experiment measures the DMI sense.

Let us take model I with an out-of-plane magnetic field which stabilized a skyrmion lattice, and now reverse the chirality of the DMI along one direction only, making  $D^x \rightarrow -D^x$ . This modified model then stabilizes an antiskyrmion

lattice. Because the skyrmion and antiskyrmion systems translate into the other only by a mirror reflection operation, their total spin-wave spectra, which are reciprocal, do not differ. However, as we have shown, the scattering rate can depend directly on the DMI orientation, and we should be able in this case to identify it.

# E. Dzyaloshinskii-Moriya interaction and spin-wave angular momentum

We saw that the nonreciprocity is seen when the probingbeam polarization, the DMI vector in reciprocal space  $\mathbf{D}(\mathbf{k})$ , and the spin wave's angular momentum align. It is easy to see that the polarization couples to the angular momentum, however, how does the angular momentum couple to the DMI? Is the angular momentum, which is the property that allows

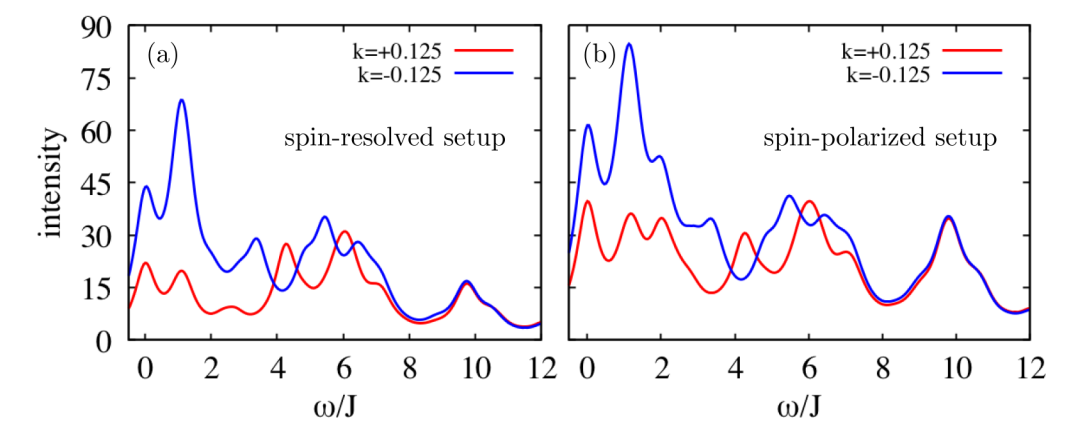


FIG. 10. Constant-wave-vector inelastic scattering spectra for a skyrmion lattice generated by model I added with an out-of-plane external magnetic field. The spectra were calculated for two opposite wave vectors  $\mathbf{k} = \pm \frac{2\pi}{a} k \,\hat{\mathbf{y}}$ . The beam polarization is along  $\hat{\mathbf{x}}$ . (a) Shows the spin-resolved setup, where only one spin-flip channel is taken (left-right scattering channel). (b) Presents the spin-polarized setup, which results from adding a spin flip and a non-spin flip (left-right + left-left scattering channels). In both cases, we can observe that the inelastic signal at  $-\mathbf{k}$  is distinct and predominantly higher than at  $\mathbf{k}$ , therefore, it is nonreciprocal. The multiple peaks correspond to the various spin-wave modes of the skyrmion lattice, in contrast to the expected single peak for a ferromagnetic phase and the three modes of a spin spiral.

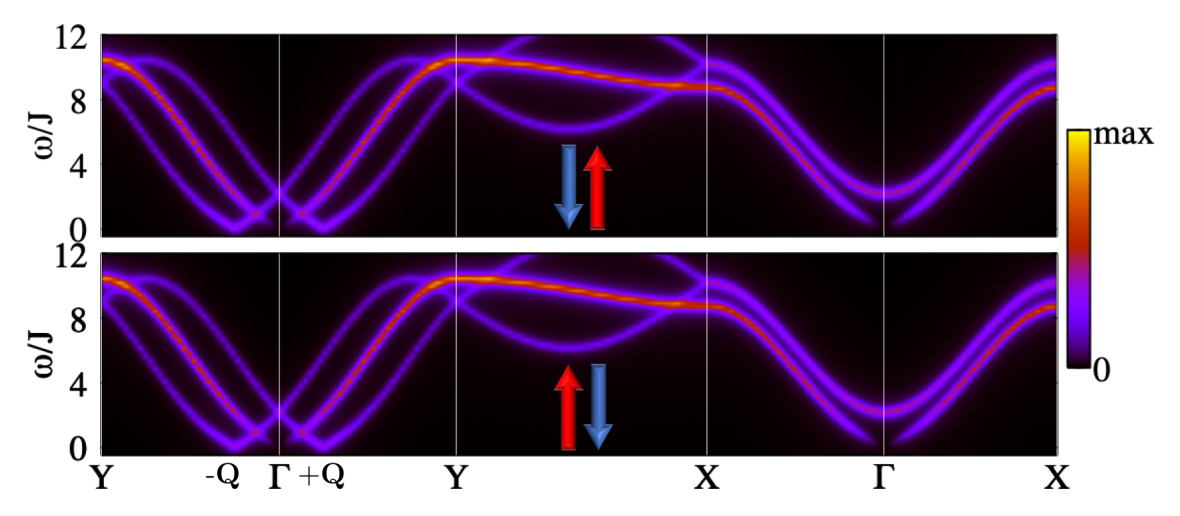


FIG. 11. Spin-resolved inelastic scattering spectra for the spin spiral generated by model I with  $D^y = 0$ . Note that the spiral itself is stabilized by  $D_x$ . The polarization is set along  $\hat{\mathbf{y}}$ , as indicated by the vertical arrows. The two spin-flip channels are degenerate and reciprocal because  $\mathbf{D}(\mathbf{k})$  has no component along the polarization to induce angular momentum of the spin-wave modes along that direction. Restoring the  $D^y$  of the original model I, a nonreciprocity occurs on the X-Γ-X while the ground-state spin configuration is not affected, proving that the DMI can directly induce the nonreciprocity of spin waves.

the nonreciprocal inelastic measurement, given by the spin structure or by the Dzyaloshinskii-Moriya interactions? The answer is that both spin configuration and the DMI set the angular momentum of the spin waves.

Let us consider model I with  $D^y$  set to zero. The same cycloidal spin spiral with  $\mathbf{Q} \parallel \hat{\mathbf{y}}$  is still the ground state. Previously, we have seen on Fig. 7(b) that spin-resolved inelastic scattering spectra for polarization along  $\hat{\mathbf{y}}$  featured nonreciprocity in the X- $\Gamma$ -X path because there  $\mathbf{D}(\mathbf{k})$  was parallel to  $\hat{\mathbf{y}}$ . Now, once  $\mathbf{D}(\mathbf{k}) = 0$  on that same path, the spectrum becomes reciprocal (see Fig. 11). This proves that the nonreciprocity is not only induced by the spin structure but also directly by the DMI. Similarly, one observes that a spin spiral stabilized by exchange interaction frustration, without involving DMI, can also feature nonreciprocity as if the DMI that could favor that structure were there [32].

We have seen that the DMI only influences the dispersion and the inelastic spectra of spin-wave modes whose angular momenta have a finite projection on D(k). An antiferromagnet hosts two counter-rotating spin-wave modes that precess in the plane perpendicular to the axis of the magnetic moments. That is why we discussed in item (iii) an example where  $\mathbf{D}(\mathbf{k})$ is parallel to this axis, which guarantees that the DMI would maximally influence the spin-wave modes. However, for a general noncollinear magnetic structure, the angular momenta of the spin waves are not obvious and, thus, only knowing the DMI structure will not be enough to predict the occurrence of the asymmetries. Our observations have shown, however, that spin structures that are energetically favored by a given component of **D**(**k**) will host spin waves whose angular momenta are along this same DMI component, i.e., they will also induce nonreciprocity to the system. We can exemplify this by taking the models I and II again, and the spin spirals that each one favors as the ground state. For model I, the cycloidal spiral with spins lying in the yz plane is stabilized by  $D^x$ , and so the angular momenta of the  $+\mathbf{Q}$  and  $-\mathbf{Q}$ modes are along  $\hat{\mathbf{x}}$ . Meanwhile, the helical spiral of model II

is stabilized by  $D^y$ , and its  $\pm \mathbf{Q}$  modes have angular momenta along  $\hat{\mathbf{v}}$ .

#### IV. CONCLUSIONS

In this paper, we contributed to the problem of mapping the Dzyaloshinskii-Moriya interaction in systems of complex magnetic structures. We did that by studying the effect of the DMI on the dynamics of spin waves using atomistic spin models. We made an important connection between the angular momentum and the chiral handedness of a spin-wave mode. Effectively, this allows us to predict when a given spin-wave mode energy and scattering rate is affected by the DMI.

We saw that the DMI can induce nonreciprocity in the spin waves. We concluded that only systems of finite magnetization can have a total spin-wave spectrum that is nonreciprocal. Nevertheless, nonreciprocity can also occur for individual spin-wave modes in systems with zero-net-magnetization and noncollinear spin textures, while the total spectrum remains reciprocal.

We showed that an external magnetic field and spinresolved energy-loss spectroscopy (SREELS), proposed in Ref. [57], can help to reveal the nonreciprocity of individual modes. We saw that only a spin-flip scattering spectrum can present nonreciprocity and that a nonreciprocal spectrum is expected when a component of D(k) is parallel to the angular momentum and the polarization of the probing electrons. As we can control the polarization of the probe beam, and the spin-resolved measurements can also determine the angular momentum of the spin waves, ultimately we can determine the DMI chirality even for zero-net-magnetization systems. This achievement is in contrast to previous expectations found on the literature [61], where other authors resorted to controlling the phase and amplitude of the probing beam to be able to determine the DMI chirality. Our findings can be generalized for other spectroscopies, such as inelastic neutron scattering and radio-frequency magnetic resonance, where the polarization of the probing particle/field can be controlled.

For the case of a skyrmion lattice, despite having a finite out-of-plane net magnetization, no component of the DMI projects along that net magnetization (which is in plane), guaranteeing that the total spin-wave spectrum is reciprocal. Nevertheless, the scattering rate still can have nonreciprocity induced by the DMI. This allowed us to detect a change in the chirality of the DMI along different directions, which permits us, for instance, to infer the existence of antiskyrmions instead of skyrmions [22].

Finally, we learned that the Dzyaloshinskii-Moriya interaction can influence the angular momentum of the spin waves directly and indirectly. In general, the DMI favors the formation of spin structures that naturally hosts spin waves whose precession axis aligns with the DMI. That is, the spin-wave angular momenta tend to be along  $\mathbf{D}(\mathbf{k})$  that favored the spin configuration in the first place. However, even those components of  $\mathbf{D}(\mathbf{k})$  that do not contribute to the energy of the ground state can directly influence the dynamics of spin waves, in particular of their angular momentum and thus their scattering rate.

#### ACKNOWLEDGMENTS

This work is supported by the Brazilian funding agency CAPES under Project No. 13703/13-7 and the European Research Council (ERC) under the European Union's Horizon 2020 research and innovation programme (ERC-consolidator Grant No. 681405-DYNASORE). We gratefully acknowledge the computing time granted by JARA-HPC on the supercomputer JURECA at Forschungszentrum Jülich and by RWTH Aachen University.

## APPENDIX: ON THE CHIRAL ASYMMETRY OF SPIN WAVES

## 1. Spin-wave chirality in ferromagnets

The only contribution in the Hamiltonian that can be sensitive to the chirality of a spin wave (see Sec. III A) is that of the Dzyaloshinskii-Moriya interaction. It goes with the cross product of two spin moments at different sites. If we consider the *ansatz* for a spin-wave snapshot given by Eq. (4), we get

$$\mathbf{S}_{i} \times \mathbf{S}_{j} = \left[ \left( S_{i}^{2} S_{j}^{0} - S_{i}^{0} S_{j}^{2} \right) \mathbf{n}^{1} + \left( S_{i}^{0} S_{j}^{1} - S_{i}^{1} S_{j}^{0} \right) \mathbf{n}^{2} + \left( S_{i}^{1} S_{j}^{2} - S_{i}^{2} S_{j}^{1} \right) \mathbf{n}^{0} \right]$$

$$= \left[ c \sin \theta \cos \theta (\sin \phi_{i} - \sin \phi_{j}) \mathbf{n}^{1} + \cos \theta \sin \theta (\cos \phi_{j} - \cos \phi_{i}) \mathbf{n}^{2} + c \sin^{2} \theta \sin \left[ \mathbf{k} \cdot (\mathbf{R}_{i} - \mathbf{R}_{i}) \right] \mathbf{n}^{0} \right]$$

$$(A1)$$

and, therefore, two terms depend on the chirality constant c. However, evaluating the sum over all lattice points required by the Hamiltonian (1), the first term vanishes:

$$\sum_{ij} D_{ij}^{1} (\sin \phi_i - \sin \phi_j) = 2D_{ij}^{1} \sin \phi_i = 0$$
 (A2)

because  $D_{ij}^1 = -D_{ii}^1$ .

Thus, the only term that depends on the spin-wave chirality in the energy, obtained by substituting the spin-wave equation of Eq. (4) into the Hamiltonian in Eq. (1), has the form

$$E(\mathbf{k}, c) = -\frac{1}{2}c \sin^2 \theta \sum_{ij} \sin[\mathbf{k} \cdot (\mathbf{R}_j - \mathbf{R}_i)] \mathbf{D}_{ij} \cdot \mathbf{n}^0$$
$$= -\frac{1}{2}c \sin^2 \theta N \mathbf{n}^0 \cdot \mathbf{D}(\mathbf{k}), \tag{A3}$$

where

$$\mathbf{D}(\mathbf{k}) = \sum_{j} \sin(\mathbf{k} \cdot \mathbf{R}_{ij}) \mathbf{D}_{ij}.$$
 (A4)

We can notice that only the D(k) component along the magnetization contributes to the chirality. This result matches the conclusion of Udvardi and Szunyogh [24].

#### 2. Spin waves in a classical approach

In this section, we solve the equation of motion for every spin in a ferromagnet to understand the dynamics of its spin waves and the corresponding local spin precession.

## a. Effective field

Considering the magnetic moments of a ferromagnet as classical vectors, their dynamics are governed by the phenomenological equation of motion given by Eq. (6). Solving this equation simultaneously for all sites provides spin-wave solutions. First, we need to determine the effective field, given by Eq. (7), which for the Hamiltonian of Eq. (1) reads as

$$B_i^{\text{eff}} = -\frac{\partial H}{\partial \mathbf{S}_i} = \sum_j (J_{ij}\mathbf{S}_j + \mathbf{S}_j \times \mathbf{D}_{ij}) + \mathbf{B}.$$
 (A5)

In calculating the derivative of the Hamiltonian, we did not have to take care of terms with k = j = i because  $J_{ij}$  and  $\mathbf{D}_{ij}$  are zero. Also, we made use of the cyclic permutation of the scalar triple product:  $\mathbf{a} \cdot (\mathbf{b} \times \mathbf{c}) = \mathbf{c} \cdot (\mathbf{a} \times \mathbf{b}) = \mathbf{b} \cdot (\mathbf{c} \times \mathbf{a})$ ; and we swapped the interaction parameters index respecting their symmetries:  $J_{ij} = J_{ji}$  and  $\mathbf{D}_{ij} = -\mathbf{D}_{ji}$ .

#### b. Equation of motion

Thus, the equation of motion in Eq. (6) reads as

$$\frac{d\mathbf{S}_{i}}{dt} = -\sum_{j} \left[ J_{ij} \left( S_{i}^{y} S_{j}^{z} - S_{i}^{z} S_{j}^{y} \right) + S_{j}^{x} (\mathbf{S}_{i} \cdot \mathbf{D}_{ij}) - D_{ij}^{x} (\mathbf{S}_{i} \cdot \mathbf{S}_{j}) \right] \hat{\mathbf{x}}$$

$$- \left( S_{i}^{y} B^{z} - S_{i}^{z} B^{y} \right) \hat{\mathbf{x}} - \sum_{j} \left[ J_{ij} \left( S_{i}^{z} S_{j}^{x} - S_{i}^{x} S_{j}^{z} \right) \right]$$

$$+ S_{j}^{y} (\mathbf{S}_{i} \cdot \mathbf{D}_{ij}) - D_{ij}^{y} (\mathbf{S}_{i} \cdot \mathbf{S}_{j}) \hat{\mathbf{y}} - \left( S_{i}^{z} B^{x} - S_{i}^{x} B^{z} \right) \hat{\mathbf{y}}$$

$$- \sum_{j} \left[ J_{ij} \left( S_{i}^{y} S_{j}^{x} - S_{i}^{x} S_{j}^{y} \right) + S_{j}^{z} (\mathbf{S}_{i} \cdot \mathbf{D}_{ij}) - D_{ij}^{z} (\mathbf{S}_{i} \cdot \mathbf{S}_{j}) \right] \hat{\mathbf{z}}$$

$$- \left( S_{i}^{x} B^{y} - S_{i}^{y} B^{x} \right) \hat{\mathbf{z}}.$$
(A6)

Let us assume a magnetic field of magnitude B along the z direction and that the motion of each spin is of a small amplitude around the equilibrium axis. This implies that we consider that  $S_i^x$ ,  $S_i^y \ll 1$ , and in first-order approximation we disregard all products between them and take  $S_i^z \sim S$ . Thus,

the above equation becomes

$$\frac{d\mathbf{S}_i}{dt} = -\left(S\sum_j \left[J_{ij}(S_i^y - S_j^y) + D_{ij}^z S_j^x\right] + BS_i^y\right)\hat{\mathbf{x}}$$

$$-\left(S\sum_j \left[J_{ij}(S_j^x - S_i^x) + D_{ij}^z S_j^y\right] - BS_i^x\right)\hat{\mathbf{y}}, \quad (A7)$$

because  $\sum_{j} D_{ij}^{x,y} = 0$  when the summation is over a Bravais lattice due to the antisymmetry of the DMI. We can see that, within the linear approximation, only the component of DMI along the magnetization matters.

This is a vectorial equation, which represents two equations: one for the *x* and one for the *y* components of the spin moment. Here note that the dynamics of one of the components depends on that of the other, therefore, we have a set of two coupled equations. Then, let us consider the following transformation:

$$S_i^+ = S_i^x + iS_i^y$$
 and  $S_i^- = S_i^x - iS_i^y$ ,  
 $S_i^x = \frac{1}{2}(S_i^+ + S_i^-)$  and  $S_i^y = \frac{1}{2i}(S_i^+ - S_i^-)$ , (A8)

which define the circular components of the spin moments, and the following definition

$$J_{ij}^{\pm} = J_{ij} \pm iD_{ij}^z. \tag{A9}$$

Applying these to Eq. (A7), we find

$$\mp i \frac{dS_i^{\pm}}{dt} = S \sum_j [J_{ij} S_i^{\pm} - J_{ij}^{\mp} S_j^{\pm}] + B S_i^{\pm}, \tag{A10}$$

defining two decoupled equations of motion.

#### c. Fourier transformation

The dynamics of a given site depends on what is happening to all sites connected to it via the exchange interaction. However, if the system has translational symmetry, we can Fourier transform these equations defining

$$S_{\mathbf{k}}^{\pm} = \frac{1}{\sqrt{N}} \sum_{i} e^{-i\mathbf{k} \cdot \mathbf{R}_{i}} S_{i}^{\pm}, \quad S_{i}^{\pm} = \frac{1}{\sqrt{N}} \sum_{\mathbf{k}} e^{i\mathbf{k} \cdot \mathbf{R}_{i}} S_{\mathbf{k}}^{\pm}. \quad (A11)$$

Then, by left multiplying Eq. (A10) with  $\frac{1}{\sqrt{N}} \sum_{i} e^{-i\mathbf{k}\cdot\mathbf{R}_{i}}$ , one gets

$$\mp i \frac{dS_{\mathbf{k}}^{\pm}(t)}{dt} = (S(J_{\mathbf{0}} - J_{\mathbf{k}}^{\mp}) + B)S_{\mathbf{k}}^{\pm}(t), \tag{A12}$$

where the Fourier-transformed interactions are defined as

$$J_{\mathbf{k}}^{\pm} = \sum_{i} e^{i\mathbf{k}\cdot\mathbf{R}_{ij}} J_{ij}^{\pm},\tag{A13}$$

which assumes a translational symmetry, such that  $J_{ij}^{\pm}$  only depends on the difference  $\mathbf{R}_{ij} = \mathbf{R}_j - \mathbf{R}_i$ . Note as well that  $J_0^{\pm} = \sum_i (J_{ij} \pm iD_{ij}^z) = \sum_i J_{ij} = J_0$ , again because of the DMI antisymmetry. Next follows some useful properties of the interactions in the reciprocal space:

$$J_{-\mathbf{k}}^{\pm} = \sum_{i} e^{-i\mathbf{k}\cdot\mathbf{R}_{ij}} J_{ij}^{\pm} = \sum_{i} e^{i\mathbf{k}\cdot\mathbf{R}_{ji}} J_{ji}^{\mp} = J_{\mathbf{k}}^{\mp}$$
(A14)

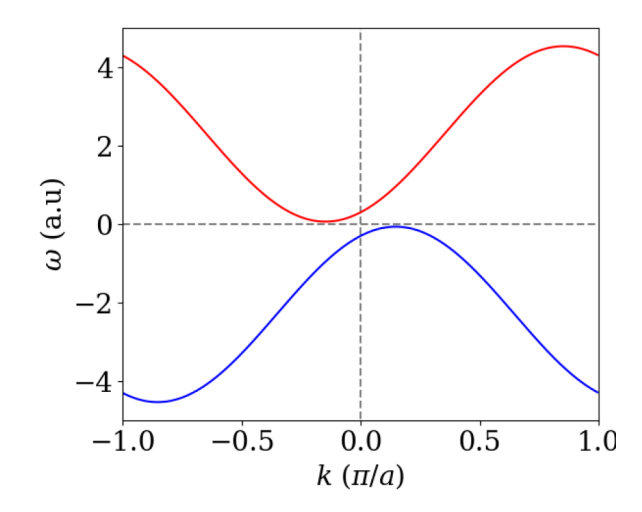


FIG. 12. Spin-wave dispersion for a ferromagnet with DMI. The red and blue curves correspond to the functions  $\omega_{\bf k}^-$  and  $\omega_{\bf k}^+$  from Eq. (A18), respectively. The blue curve is obtained from the red one by time reversal, which enforces  $\omega_{\bf k}^+ = -\omega_{-\bf k}^-$ . Parameters: J=1,  $D^z=0.5$ , B=0.3.

and

$$J_{\mathbf{k}}^{\pm} = \sum_{i} (\cos(\mathbf{k} \cdot \mathbf{R}_{ij}) + i \sin(\mathbf{k} \cdot \mathbf{R}_{ij})) (J_{ij} \pm i D_{ij}^{z})$$
$$= \sum_{i} A_{ij} \cos(\mathbf{k} \cdot \mathbf{R}_{ij} \pm \theta_{ij}), \tag{A15}$$

where  $\theta_{ij} = \arctan(D_{ij}^z/J_{ij})$  and  $A_{ij} = \sqrt{(D_{ij}^z)^2 + (J_{ij})^2}$ . The last equation shows that  $J_{\mathbf{k}}^{\pm}$  is purely real and that it can be expanded in terms of cosine functions whose phase is given by the magnetic exchange and DMI ratio. This derives from the fact that the sum of a Bravais lattice of an antisymmetric function vanishes,  $\sum_i \sin(\mathbf{k} \cdot \mathbf{R}_{ij}) J_{ij} = \sum_i \cos(\mathbf{k} \cdot \mathbf{R}_{ij}) D_{ij}^z = 0$ .

#### d. Eigenvalues: The frequencies

The differential equations in (A12) have solutions of the type

$$S_{\mathbf{k}}^{\pm}(t) = S_{\mathbf{k}}^{\pm} e^{-i\omega_{\mathbf{k}}^{\pm}t},\tag{A16}$$

which plugging into Eq. (A12) results in

$$\mp \omega_{\mathbf{k}}^{\pm} S_{\mathbf{k}}^{\pm} = (S(J_{\mathbf{0}} - J_{\mathbf{k}}^{\mp}) + B) S_{\mathbf{k}}^{\pm}$$
 (A17)

and, therefore, the eigenvalues of these equations that correspond to the solution frequencies are given by

$$\omega_{\mathbf{k}}^{\pm} = \mp (S(J_0 - J_{\mathbf{k}}^{\mp}) + B).$$
 (A18)

For a one-dimensional ferromagnet with nearest-neighboronly MEI and DMI, J = 1,  $D^z = 0.5$ , and a magnetic field B = 0.3, we plotted the above equation in Fig. 12.

Using Eq. (A14), we can notice that

$$\omega_{-\mathbf{k}}^{\pm} = \mp [S(J_0 - J_{\mathbf{k}}^{\pm}) + B] = -\omega_{\mathbf{k}}^{\mp},$$
 (A19)

that is, the frequency of each solution is related to the other by an inversion of wave vector and a sign change of the frequency, which can be translated into an inversion of time in Eq. (A16) (see Fig. 12). Due to  $J_0^{\pm} = J_0$ , we have that

 $\omega_{\bf k}^{\pm} \to \mp B$  when  ${\bf k} \to 0$ . Similarly, Eq. (A17) can be used to show that the eigenvectors satisfy  $S_{-{\bf k}}^{\pm} = (S_{\bf k}^{\mp})^*$ .

In the absence of DMI, and if  $J_{ij} > 0$ , we have that  $\omega_{\bf k}^{\pm} = \omega_{-{\bf k}}^{\pm} = \pm \omega_{\bf k}$ , which imply that the frequencies are reciprocally symmetric and additive inverse of each other. Furthermore,  $\omega_{\mathbf{k}}$  is always real and positive, as we expect for a ferromagnetic system:

$$\omega_{\mathbf{k}} = S \sum_{i} [1 - \cos(\mathbf{k} \cdot \mathbf{R}_{ij})] J_{ij} + B > 0.$$
 (A20)

For nonzero  $D_{ij}^z$ , the phases of the cosines change, making the spin-wave dispersion nonreciprocal.

## e. Local spin dynamics

Now, it is time to transform back, from the circular components to the Cartesian ones in order to understand the precession of individual spins. For a given wave vector  $\mathbf{k}$  and using Eq. (A16) (for our purposes we can set  $S_k^{\pm} = 1$  without loss of generality), we have that

$$S_i^{\pm}(\mathbf{k}, t) = \frac{1}{\sqrt{N}} e^{i\mathbf{k}\cdot\mathbf{R}_i} S_{\mathbf{k}}^{\pm}(t) = \frac{1}{\sqrt{N}} [\cos(\mathbf{k}\cdot\mathbf{R}_i - \omega_{\mathbf{k}}^{\pm}t) + i\sin(\mathbf{k}\cdot\mathbf{R}_i - \omega_{\mathbf{k}}^{\pm}t)]. \tag{A21}$$

Comparing these equations with their definitions at Eq. (A8) in terms of the Cartesian components  $S_i^{\pm} = S_i^x \pm iS_i^y$ , we get a solution for each equation:

$$S_{\mathbf{k}}^{+}(t) \to \begin{pmatrix} S_{i}^{x}(\mathbf{k}, t) \\ S_{i}^{y}(\mathbf{k}, t) \end{pmatrix} = \frac{1}{\sqrt{N}} \begin{pmatrix} \cos(\mathbf{k} \cdot \mathbf{R}_{i} - \omega_{\mathbf{k}}^{+} t) \\ \sin(\mathbf{k} \cdot \mathbf{R}_{i} - \omega_{\mathbf{k}}^{+} t) \end{pmatrix},$$

$$S_{\mathbf{k}}^{-}(t) \to \begin{pmatrix} S_{i}^{x}(\mathbf{k}, t) \\ S_{i}^{y}(\mathbf{k}, t) \end{pmatrix} = \frac{1}{\sqrt{N}} \begin{pmatrix} \cos(\mathbf{k} \cdot \mathbf{R}_{i} - \omega_{\mathbf{k}}^{-} t) \\ -\sin(\mathbf{k} \cdot \mathbf{R}_{i} - \omega_{\mathbf{k}}^{-} t) \end{pmatrix}.$$
(A22)

- [1] P. W. Anderson, More is different, Science 177, 393 (1972).
- [2] I. Dzyaloshinsky, A thermodynamic theory of "weak" ferromagnetism of antiferromagnetics, J. Phys. Chem. Solids 4, 241 (1958).
- [3] T. Moriya, Anisotropic superexchange interaction and weak ferromagnetism, Phys. Rev. 120, 91 (1960).
- [4] M. Bode, M. Heide, K. von Bergmann, P. Ferriani, S. Heinze, G. Bihlmayer, A. Kubetzka, O. Pietzsch, S. Blügel, and R. Wiesendanger, Chiral magnetic order at surfaces driven by inversion asymmetry, Nature (London) 447, 190 (2007).
- [5] P. Ferriani, K. von Bergmann, E. Y. Vedmedenko, S. Heinze, M. Bode, M. Heide, G. Bihlmayer, S. Blügel, and R. Wiesendanger, Atomic-Scale Spin Spiral with a Unique Rotational Sense: Mn Monolayer on W(001), Phys. Rev. Lett. 101, 027201 (2008).
- [6] Y. Onose, T. Ideue, H. Katsura, Y. Shiomi, N. Nagaosa, and Y. Tokura, Observation of the magnon hall effect, Science 329, 297 (2010).
- [7] K.-S. Ryu, L. Thomas, S.-H. Yang, and S. Parkin, Chiral spin torque at magnetic domain walls, Nat. Nanotechnol. 8, 527
- [8] S. Emori, U. Bauer, S.-M. Ahn, E. Martinez, and G. S. D. Beach, Current-driven dynamics of chiral ferromagnetic domain walls, Nat. Mater. 12, 611 (2013).

We can show that these two equations are equivalent by using the relation derived in Eq. (A19). Doing so, we can rewrite the second solution in Eq. (A22) to get

$$\begin{pmatrix} S_i^x(-\mathbf{k},t) \\ S_i^y(-\mathbf{k},t) \end{pmatrix} = \frac{1}{\sqrt{N}} \begin{pmatrix} \cos(\mathbf{k} \cdot \mathbf{R}_i - \omega_{\mathbf{k}}^+ t) \\ \sin(\mathbf{k} \cdot \mathbf{R}_i - \omega_{\mathbf{k}}^+ t) \end{pmatrix}, \tag{A23}$$

which is equivalent to the first solution in Eq. (A22) but with opposite wave vector. These solutions represent counterclockwise circular precessions.

#### 3. Circular components duality

The following reviews the duality between the circular components of the spin moments and how they evolve through the transformation considered previously, such as the Fourier transformation.

From the definition of the circular components in Eq. (A8), we have that

$$(S_i^{\pm})^* = S_i^{\mp}, \tag{A24}$$

that is, one is the complex conjugate of the other. Given the Fourier transformation definitions by Eq. (A11), the complexconjugate duality of the Fourier counterparts is given by

$$(S_{\mathbf{k}}^{\pm})^* = S_{-\mathbf{k}}^{\mp}.$$
 (A25)

 $(S_{\mathbf{k}}^{\pm})^* = S_{-\mathbf{k}}^{\mp}.$  (A25) Given the definition of the time evolution, Eq. (A16), we have

$$(S_{\mathbf{k}}^{\pm}(t))^* = S_{-\mathbf{k}}^{\mp}(-t).$$
 (A26)

And again, we see that they are related by a time-reversal operation.

- [9] M. Jamali, J. H. Kwon, S.-M. Seo, K.-J. Lee, and H. Yang, Spin wave nonreciprocity for logic device applications, Sci. Rep. 3, 3160 (2013).
- [10] F. Garcia-Sanchez, P. Borys, A. Vansteenkiste, J.-V. Kim, and R. L. Stamps, Nonreciprocal spin-wave channeling along textures driven by the Dzyaloshinskii-Moriya interaction, Phys. Rev. B 89, 224408 (2014).
- [11] F. Garcia-Sanchez, P. Borys, R. Soucaille, J.-P. Adam, R. L. Stamps, and J.-V. Kim, Narrow Magnonic Waveguides Based on Domain Walls, Phys. Rev. Lett. 114, 247206 (2015).
- [12] A. Fert, V. Cros, and J. Sampaio, Skyrmions on the track, Nat. Nanotechnol. 8, 152 (2013).
- [13] J. Sampaio, V. Cros, S. Rohart, A. Thiaville, and A. Fert, Nucleation, stability and current-induced motion of isolated magnetic skyrmions in nanostructures, Nat. Nanotechnol. 8, 839 (2013).
- [14] R. Tomasello, E. Martinez, R. Zivieri, L. Torres, M. Carpentieri, and G. Finocchio, A strategy for the design of skyrmion racetrack memories, Sci. Rep. 4, 6784 (2014).
- [15] D. M. Crum, M. Bouhassoune, J. Bouaziz, B. Schweflinghaus, S. Blügel, and S. Lounis, Perpendicular reading of single confined magnetic skyrmions, Nat. Commun. 6, 8541 (2015).
- [16] M. Garst, J. Waizner, and D. Grundler, Collective spin excitations of helices and magnetic skyrmions: Review and

- perspectives of magnonics in non-centrosymmetric magnets, J. Phys. D: Appl. Phys. **50**, 293002 (2017).
- [17] L. Rózsa, J. Hagemeister, E. Y. Vedmedenko, and R. Wiesendanger, Effective damping enhancement in noncollinear spin structures, Phys. Rev. B 98, 100404(R) (2018).
- [18] S. A. Díaz, J. Klinovaja, and D. Loss, Topological Magnons and Edge States in Antiferromagnetic Skyrmion Crystals, Phys. Rev. Lett. 122, 187203 (2019).
- [19] N. Nagaosa and Y. Tokura, Topological properties and dynamics of magnetic skyrmions, Nat. Nanotechnol. 8, 899 (2013).
- [20] N. Bogdanov and D. A. Yablonskii, Thermodynamically stable "vortices" in magnetically ordered crystals. The mixed state of magnets, J. Exp. Theor. Phys. 95, 178 (1989) [Sov. Phys. JETP 68, 101 (1989)].
- [21] U. K. Rößler, A. N. Bogdanov, and C. Pfleiderer, Spontaneous skyrmion ground states in magnetic metals, Nature (London) 442, 797 (2006).
- [22] M. Hoffmann, B. Zimmermann, G. P. Müller, D. Schürhoff, N. S. Kiselev, C. Melcher, and S. Blügel, Antiskyrmions stabilized at interfaces by anisotropic Dzyaloshinskii-Moriya interactions, Nat. Commun. 8, 308 (2017).
- [23] S.-W. Cheong, D. Talbayev, V. Kiryukhin, and A. Saxena, Broken symmetries, non-reciprocity, and multiferroicity, njp Quantum Mater. 3, 19 (2018).
- [24] L. Udvardi and L. Szunyogh, Chiral Asymmetry of the Spin-Wave Spectra in Ultrathin Magnetic Films, Phys. Rev. Lett. 102, 207204 (2009).
- [25] A. T. Costa, R. B. Muniz, S. Lounis, A. B. Klautau, and D. L. Mills, Spin-orbit coupling and spin waves in ultrathin ferromagnets: The spin-wave Rashba effect, Phys. Rev. B 82, 014428 (2010).
- [26] J.-H. Moon, S.-M. Seo, K.-J. Lee, K.-W. Kim, J. Ryu, H.-W. Lee, R. D. McMichael, and M. D. Stiles, Spin-wave propagation in the presence of interfacial Dzyaloshinskii-Moriya interaction, Phys. Rev. B 88, 184404 (2013).
- [27] D. Cortés-Ortuño and P. Landeros, Influence of the Dzyaloshinskii-Moriya interaction on the spin-wave spectra of thin films, J. Phys.: Condens. Matter 25, 156001 (2013).
- [28] M. Kostylev, Interface boundary conditions for dynamic magnetization and spin wave dynamics in a ferromagnetic layer with the interface Dzyaloshinskii-Moriya interaction, J. Appl. Phys. 115, 233902 (2014).
- [29] R. W. Damon and J. R. Eshbach, Magnetostatic modes of a ferromagnet slab, J. Phys. Chem. Solids 19, 308 (1961).
- [30] *Surface Excitations*, Modern problems in condensed matter sciences, Vol. 9, edited by V. M. Agranovich and Rodney Loudon (North-Holland, Amsterdam, 1984), Chap. 3.
- [31] K. Yamamoto, G. C. Thiang, P. Pirro, K.-W. Kim, K. Everschor-Sitte, and E. Saitoh, Topological Characterization of Classical Waves: The Topological Origin of Magnetostatic Surface Spin Waves, Phys. Rev. Lett. 122, 217201 (2019).
- [32] S. Cheon, H.-W. Lee, and S.-W. Cheong, Nonreciprocal spin waves in a chiral antiferromagnet without the Dzyaloshinskii-Moriya interaction, Phys. Rev. B **98**, 184405 (2018).
- [33] Kh. Zakeri, Y. Zhang, J. Prokop, T.-H. Chuang, N. Sakr, W. X. Tang, and J. Kirschner, Asymmetric Spin-Wave Dispersion on Fe(110): Direct Evidence of the Dzyaloshinskii-Moriya Interaction, Phys. Rev. Lett. 104, 137203 (2010).

- [34] M. Plihal, D. L. Mills, and J. Kirschner, Spin Wave Signature in the Spin Polarized Electron Energy Loss Spectrum of Ultrathin Fe Films: Theory and Experiment, Phys. Rev. Lett. 82, 2579 (1999).
- [35] R. Vollmer, M. Etzkorn, P. S. A. Kumar, H. Ibach, and J. Kirschner, Spin-Polarized Electron Energy Loss Spectroscopy of High Energy, Large Wave Vector Spin Waves in Ultrathin fcc Co Films on Cu(001), Phys. Rev. Lett. 91, 147201 (2003).
- [36] E. Michel, H. Ibach, and C. M. Schneider, Spin waves in ultrathin hexagonal cobalt films on W(110), Cu(111), and Au(111) surfaces, Phys. Rev. B **92**, 024407 (2015).
- [37] E. Michel, H. Ibach, and C. M. Schneider, High resolution electron energy loss spectroscopy of spin waves in ultra-thin cobalt films, Surf. Interface Anal. 48, 1104 (2016).
- [38] F. J. dos Santos, M. dos Santos Dias, and S. Lounis, First-principles investigation of spin-wave dispersions in surface-reconstructed Co thin films on W(110), Phys. Rev. B 95, 134408 (2017).
- [39] J. Cho, N.-H. Kim, S. Lee, J.-S. Kim, R. Lavrijsen, A. Solignac, Y. Yin, D.-S. Han, N. J. J. van Hoof, H. J. M. Swagten, B. Koopmans, and C.-Y. You, Thickness dependence of the interfacial Dzyaloshinskii-Moriya interaction in inversion symmetry broken systems, Nat. Commun. 6, 7635 (2015).
- [40] K. Di, V. L. Zhang, H. S. Lim, S. C. Ng, M. H. Kuok, J. Yu, J. Yoon, X. Qiu, and H. Yang, Direct Observation of the Dzyaloshinskii-Moriya Interaction in a Pt/Co/Ni Film, Phys. Rev. Lett. 114, 047201 (2015).
- [41] H. T. Nembach, J. M. Shaw, M. Weiler, E. Jué, and T. J. Silva, Linear relation between Heisenberg exchange and interfacial Dzyaloshinskii-Moriya interaction in metal films, Nat. Phys. 11, 825 (2015).
- [42] M. Belmeguenai, J.-P. Adam, Y. Roussigné, S. Eimer, T. Devolder, J.-V. Kim, S. M. Cherif, A. Stashkevich, and A. Thiaville, Interfacial Dzyaloshinskii-Moriya interaction in perpendicularly magnetized Pt/Co/AlO<sub>x</sub> ultrathin films measured by Brillouin light spectroscopy, Phys. Rev. B 91, 180405(R) (2015).
- [43] S. Tacchi, R. E. Troncoso, M. Ahlberg, G. Gubbiotti, M. Madami, J. Åkerman, and P. Landeros, Interfacial Dzyaloshinskii-Moriya Interaction in Pt/CoFeB Films: Effect of the Heavy-Metal Thickness, Phys. Rev. Lett. 118, 147201 (2017).
- [44] L. Camosi, S. Rohart, O. Fruchart, S. Pizzini, M. Belmeguenai, Y. Roussigné, A. Stashkevich, S. M. Cherif, L. Ranno, M. de Santis, and J. Vogel, Anisotropic Dzyaloshinskii-Moriya interaction in ultrathin epitaxial Au/Co/W(110), Phys. Rev. B 95, 214422 (2017).
- [45] T. J. Sato, D. Okuyama, T. Hong, A. Kikkawa, Y. Taguchi, T.-h. Arima, and Y. Tokura, Magnon dispersion shift in the induced ferromagnetic phase of noncentrosymmetric MnSi, Phys. Rev. B 94, 144420 (2016).
- [46] T. Weber, J. Waizner, G. S. Tucker, R. Georgii, M. Kugler, A. Bauer, C. Pfleiderer, M. Garst, and P. Böni, Field dependence of nonreciprocal magnons in chiral MnSi, Phys. Rev. B 97, 224403 (2018).
- [47] T. Weber, J. Waizner, G. S. Tucker, L. Beddrich, M. Skoulatos, R. Georgii, A. Bauer, C. Pfleiderer, M. Garst, and P. Böni, Nonreciprocal magnons in non-centrosymmetric MnSi, AIP Adv. 8, 101328 (2018).

- [48] T. Weber, J. Waizner, P. Steffens, A. Bauer, C. Pfleiderer, M. Garst, and P. Böni, Polarized inelastic neutron scattering of non-reciprocal spin waves in MnSi, Phys. Rev. B 100, 060404(R) (2019).
- [49] T. Schwarze, J. Waizner, M. Garst, A. Bauer, I. Stasinopoulos, H. Berger, C. Pfleiderer, and D. Grundler, Universal helimagnon and skyrmion excitations in metallic, semiconducting and insulating chiral magnets, Nat. Mater. 14, 478 (2015).
- [50] Y. Iguchi, S. Uemura, K. Ueno, and Y. Onose, Nonreciprocal magnon propagation in a noncentrosymmetric ferromagnet LiFe<sub>5</sub>O<sub>8</sub>, Phys. Rev. B **92**, 184419 (2015).
- [51] S. Seki, Y. Okamura, K. Kondou, K. Shibata, M. Kubota, R. Takagi, F. Kagawa, M. Kawasaki, G. Tatara, Y. Otani, and Y. Tokura, Magnetochiral nonreciprocity of volume spin wave propagation in chiral-lattice ferromagnets, Phys. Rev. B 93, 235131 (2016).
- [52] J. H. Kwon, J. Yoon, P. Deorani, J. M. Lee, J. Sinha, K.-J. Lee, M. Hayashi, and H. Yang, Giant nonreciprocal emission of spin waves in Ta/Py bilayers, Sci. Adv. 2, e1501892 (2016).
- [53] J. M. Lee, C. Jang, B.-C. Min, S.-W. Lee, K.-J. Lee, and J. Chang, All-electrical measurement of interfacial Dzyaloshinskii-Moriya interaction using collective spin-wave dynamics, Nano Lett. 16, 62 (2016).
- [54] J. Lucassen, C. F. Schippers, M. A. Verheijen, P. Fritsch, E. J. Geluk, B. Barcones, R. A. Duine, S. Wurmehl, H. J. M. Swagten, B. Koopmans, and R. Lavrijsen, Extraction

- of Dzyaloshinskii-Moriya interaction from propagating spin waves, Phys. Rev. B **101**, 064432 (2020).
- [55] S. Seki, M. Garst, J. Waizner, R. Takagi, N. D. Khanh, Y. Okamura, K. Kondou, F. Kagawa, Y. Otani, and Y. Tokura, Propagation dynamics of spin excitations along skyrmion strings, Nat. Commun. 11, 256 (2020).
- [56] G. Gitgeatpong, Y. Zhao, P. Piyawongwatthana, Y. Qiu, L. W. Harriger, N. P. Butch, T. J. Sato, and K. Matan, Nonreciprocal Magnons and Symmetry-Breaking in the Noncentrosymmetric Antiferromagnet, Phys. Rev. Lett. 119, 047201 (2017).
- [57] F. J. dos Santos, M. dos Santos Dias, F. S. M. Guimarães, J. Bouaziz, and S. Lounis, Spin-resolved inelastic electron scattering by spin waves in noncollinear magnets, Phys. Rev. B 97, 024431 (2018).
- [58] G. P. Müller, M. Hoffmann, C. Dißelkamp, D. Schürhoff, S. Mavros, M. Sallermann, N. S. Kiselev, H. Jónsson, and S. Blügel, Spirit: Multifunctional framework for atomistic spin simulations, Phys. Rev. B 99, 224414 (2019).
- [59] Roger S. K. Mong, A. M. Essin, and J. E. Moore, Antiferromagnetic topological insulators, Phys. Rev. B 81, 245209 (2010).
- [60] F. J. dos Santos, M. dos S. Dias, and S. Lounis, Modelling spin waves in noncollinear antiferromagnets: Spin-flop states, spin spirals, skyrmions and antiskyrmions, arXiv:2005.07250.
- [61] V. E. Dmitrienko, E. N. Ovchinnikova, S. P. Collins, G. Nisbet, G. Beutier, Y. O. Kvashnin, V. V. Mazurenko, A. I. Lichtenstein, and M. I. Katsnelson, Measuring the Dzyaloshinskii-Moriya interaction in a weak ferromagnet, Nat. Phys. 10, 202 (2014).